Biomaterials Science

ROYAL SOCIETY OF CHEMISTRY

REVIEW

View Article Online
View Journal | View Issue

Cite this: *Biomater. Sci.*, 2025, **13**, 1379

Living material-derived intelligent micro/nanorobots

Shuhuai Wang, Ya Liu, Shuangjiao Sun, Qinyi Gui, Wei Liu * and Wei Long *

Received 18th December 2024,
Accepted 27th January 2025

DOI: 10.1039/d4bm01685h

rsc.li/biomaterials-science

Living materials, which include various types of cells, organelles, and biological components from animals, plants, and microorganisms, have become central to recent investigations in micro and nanorobotics. Living material-derived intelligent micro/nanorobots (LMNRs) are self-propelled devices that combine living materials with synthetic materials. By harnessing energy from external physical fields or biological sources, LMNRs can move autonomously and perform various biomedical functions, such as drug delivery, crossing biological barriers, medical imaging, and disease treatment. This review, from a biomimetic strategy perspective, summarized the latest advances in the design and biomedical applications of LMNRs. It provided a comprehensive overview of the living materials used to construct LMNRs, including mammalian cells, plants, and microorganisms while highlighting their biological properties and functions. Lastly, the review discussed the major challenges in this field and offered suggestions for future research that may help facilitate the clinical application of LMNRs in the near future.

1. Introduction

Micro/nanorobots (MNRs) are tiny devices that can move and work purposefully by converting different forms of energy into physical motion.[1,2] Over the past two decades, by virtue of increasing nanotechnologies, various MNRs with distinct structures (*e.g.* wires, tubes, bowls, and Janus)[3] and propulsion modes have been developed.[4–6] The propulsion of MNRs is the basis for their movement. Various types of engines/motors have been developed, including chemical engines that utilize catalytic reactions, magnetic engines that respond to external magnetic fields, acoustic engines driven by ultrasound waves, and biological engines that harness the motility of living cells or microorganisms. These engines enable MNRs to swim in biological environments, deliver therapeutic agents to specific targets, and perform tasks with high precision and efficiency. The versatile MNRs provide diverse alternatives for applications in the biomedical world, including drug delivery,[7] medical diagnosis,[8] noninvasive surgery,[9] and biosensing.[10] However, as we know, the material type, size, shape, and surface properties will influence the stability and functionalities of MNRs, especially when they are used *in vivo*. On the other hand, MNRs can interact with or be adsorbed by proteins or cells. It would affect body health or even cause adverse effects such as immune response, inflammation, or body toxicity. Besides, MNRs are fragile to the oxidation or reduction microenvironment, and therefore lose their stability.[11] To overcome the above challenges for biomedical-used MNRs, it is necessary to design MNRs from a biomimetic perspective, which enables MNRs to adapt to an *in vivo* environment.[12] For instance, the cell membrane-coating strategy protects MNRs from immune detection, enhancing biocompatibility and stability while diminishing inflammatory responses.[13] These biomimetic approaches allow MNRs to function effectively in physiological environments by imitating natural cellular entities.

Living material-derived micro/nanorobots (LMNRs) are defined as microscale or nanoscale devices that integrate living biological entities, such as mammalian cells, microorganisms, or plant-based cells, with synthetic components to achieve autonomous or externally guided motion. These LMNRs leverage the intrinsic properties of living materials, such as their motility, target recognition, or biological responsiveness, to perform specific tasks, including drug delivery, barrier penetration, or imaging, in complex environments.[14–16] By coating with cell membranes *via* co-extrusion or self-assembly techniques, LMNRs can be obtained with high biocompatibility, immune evasion, and target recognition abilities.[17] Moreover, living cells such as macrophages and neutrophils with phagocytic and migratory abilities can be utilized to engulf MNRs, forming "Trojan horses" for drug delivery and immunotherapy. According to the difference in living materials, LMNRs can be generally classified into three types

Tianjin Key Laboratory of Radiation Medicine and Molecular Nuclear Medicine, Institute of Radiation Medicine, Chinese Academy of Medical Sciences and Peking Union Medical College, Tianjin 300192, China. E-mail: liuwei@irm-cams.ac.cn, longway@irm-cams.ac.cn

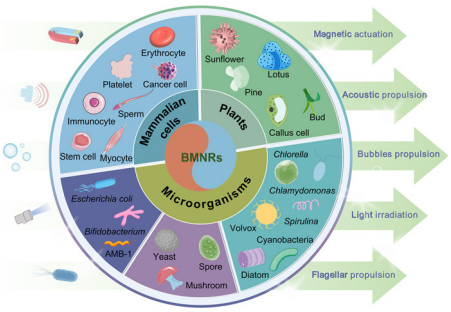

Fig. 1 Schematic overview of LMNRs based on living materials, including mammalian cells, plants, and microorganisms (microalgae, fungus, and bacterium).

including mammalian cells, plants, and microorganism-hybrid LMNRs (Fig. 1).

In this review, we systemically summarize the recent advances in the design and biomedical applications of LMNRs including drug delivery, biological barrier crossing, medical imaging, and disease treatment. Moreover, the challenges and future research opportunities are discussed, which would provide a comprehensive reference for researchers and facilitate the clinical translation of LMNRs. Herein, this review distinguishes itself by emphasizing the biomimetic design and unique integration of living materials with synthetic components. Specifically, this review systematically categorizes LMNRs based on the type of living material used, including mammalian cells, plants, and microorganisms, and provides a discussion on their *in vivo* applications. By offering a comprehensive and application-driven perspective, this review bridges critical gaps in the current literature and aims to guide future research in this evolving field.

2. LMNRs based on mammalian cells

Living material-based micro/nanorobots (LMNRs) encompass a wide range of biological entities, each offering unique benefits for specific applications. Notably, mammalian cells are prominent candidates due to their physiological properties and compatibility with the human body. Recently, natural mammalian cells were widely employed to create cell-like MNRs by integrating these cells with artificial materials.[18] These LMNRs show high biocompatibility and adaptability to physiological environments because they are similar to living cells. Cell-like MNRs can serve as cell-based propulsion systems or transporters by taking advantage of the cell autonomic movement.[19] In contrast to other MNRs, these LMNRs can utilize their intrinsic homing and chemotaxis abilities, which makes them adept at navigating or targeting diseased tissues/cells *in vivo*.[17] The following sections mainly focus on MNRs derived from mammalian cells, such as red blood cells, platelets, macrophages, cancer cells, mesenchymal stem cells, and contractile cells, highlighting their roles in the field of MNRs (Table 1).

2.1. Red blood cells

Due to the unique biconcave shape, red blood cells (RBCs) are ideal candidate materials for MNR design.[14] To make sure the MNRs have high biocompatibility, traditionally, researchers usually camouflaged them with the RBC membrane.[20] Actually, intact RBCs can also be used to create living micromotors. Zhu *et al.* fabricated RBC micromotors by incorporating magnetic NPs within erythrocytes. Under the guidance of magnetic fields, the RBC micromotors can be navigated to circulate, accumulate, and penetrate the biological body.[21] Furthermore, by exploiting the optical force exerted on the RBCs, Chen *et al.* demonstrated that RBC-based LMNRs can rotate in a clockwise direction.[22] Based on this foundational work, Liu *et al.* integrated RBCs with programmable scanning optical tweezers to assemble pentagon-shaped micromotors (Fig. 2A).[23] Controlling the rotation of these micromotors will induce a desired microflow field in the surrounding area. By precisely manipulating this microflow field, various blood cells, including platelets, WBCs, and nanodrugs, can be directed toward sites of vascular injury or cellular debris, facilitating dynamic hemostasis and targeted debris clearance.

2.2. Platelets

The receptors on the surface make platelets (PLTs) extremely sensitive to changes in the microenvironment. A notable example is the overexpression of P-selectin on platelet membranes, which facilitates PLT aggregation around the tumor site through interaction with CD44 overexpressed on cancer cells.[24] In a recently reported research study, enzyme-driven Janus PLT micromotors (JPL-motors) were developed by Tang *et al.*[25] The JPL-motors were engineered by asymmetrically immobilizing urease onto the surface of natural platelets *via* a biotin–streptavidin–biotin binding interaction. Through the catalytic decomposition of urea in biofluids, these micromotors produce NH_3 and CO_2, which can drive the JPL motors at speeds up to 1.62 times faster than non-Janus PLTs at 200 mM urea concentration. This enhanced speed significantly improves their adhesion to tumor cells. In the radiation therapy field, Liu *et al.* constructed urease-powered micromotors (PLT@Au@Urease) by *in situ* synthesis of radiosensitizer gold NPs within platelets (Fig. 2B).[26,27] The locomotion of these powered PLTs, with an average diffusion coefficient of 2.50 $\mu m^2\ s^{-1}$ at 200 mM urea concentration, significantly boosted the cellular uptake and deep penetration of gold nanoparticles and enhanced antitumor effects in combination with radiotherapy.

2.3. Immune cells

The human immune system is a complex network tasked with the critical role of distinguishing self from nonself, thereby eradicating pathogens and diseased cells. This innate immunity is the first line of defense against pathogen exposure, implemented by phagocytes, including macrophages, DCs, NK cells, and neutrophils.[28] In recent years, the unique intrinsic properties of immune cells have been employed to engineer

Table 1 Summary of LMNRs based on mammalian cells

Category	Size	Composition	Motion mechanism	Applications	Ref.
Red blood cells	2.1 ± 0.3 μm	Fe_3O_4/ICG	Magnetic actuation, acoustic propulsion	Active oxygen and photosensitizers (PSs) delivery for enhanced PDT	40
	5 μm	CHI/Hep/Au	Thermophoresis under near-infrared irradiation	Thrombus therapy with PTT	41
	400 nm, 2 μm	PFC/AuNW	Acoustic propulsion	Active intracellular oxygen delivery to hypoxic cells	42
	20 ± 5 μm	Mg/TiO_2/CHI/Eudragit	Reaction between Mg and H_2O	Oral antivirulence vaccine	43
	400 nm, 2 μm	PLT/AuNW	Acoustic propulsion	Biodetoxification	44
	4.27 ± 0.43 μm	Pt	Decomposition of H_2O_2 by catalase	—	45
	2.1 μm	Fe_3O_4/Hemoglobin	Magnetic actuation, acoustic propulsion	Active oxygen delivery	46
	9.0 ± 0.3 μm	Fe_3O_4/DOX	Magnetic actuation	Drug delivery and image-guided therapy for tumor treatment	47
Platelets	200 nm	MS/Pt/UK/Hep	Thermophoresis under near-infrared irradiation	Thrombus therapy with reduced side effects	48
	450 nm	MS/Pt/PTX/anti-VCAM-1	Thermophoresis under near-infrared irradiation	Active drug delivery of atherosclerosis treatment combined with PTT	49
	400 nm, 5 μm	Ni/Au/Pd nanohelices	Magnetic actuation	Biodetoxification	50
	2 μm	PDA/DOX	Thermophoresis under near-infrared irradiation	Combined photothermal therapy and chemotherapy for tumor ablation	24
	1.4–2.6 μm	Urease/DOX/CIP	Decomposition of urea by urease	Targeted drug delivery to cancer cells and bacteria	25
Macrophages	~20 μm	CA-MNPs/DOX-TSLPs	Magnetic actuation, chemotaxis	Photothermal chemotherapy	51
	~20 μm	Fe_2O_3	Magnetic actuation	Precise control and manipulation	29
	~20 μm	PTX/MNP-DLs	Magnetic actuation, chemotaxis	Photothermal chemotherapy	52
	~20 μm	Fe_3O_4/DOX/ICG	Magnetic actuation, chemotaxis	Photothermal chemotherapy	53
	~30 μm	Mg/TiO_2	Mg reacts with stomach acid to produce H_2	Endotoxin neutralization	54
	8–10 μm	Fe_3O_4/PDA/MnO_2/Au	Magnetic actuation, decomposition of H_2O_2 by catalase	Multi-scale bio-targets	55
	~20 μm	FePt/LPS	Magnetic actuation	Targeted cancer immunotherapy	56
	~10 μm	MnO_2/curcumin	Decomposition of H_2O_2 by catalase	Acute inflammation alleviation and immunoregulation	30
	~20 μm	SPIONs	Acoustic propulsion	Tumor penetration	57
T cells	~10 μm	SN-38	Intrinsic lymph node–homing capability	Chemotherapy for lymphoma	58
	~10 μm	Anti-CD3/CD28 antibodies	Magnetic actuation, acoustic propulsion	Cancer immunotherapies with *in situ* T-cell immunoactivation	32
Cancer cells	240 nm	mC@SiO_2@DOX	Thermophoresis under near-infrared irradiation	Synergistic photothermal chemotherapy for breast cancer	59
	2 μm	Au/$CaCO_3$/DOX	Acoustic propulsion	Immune stimulation	60
	180 nm	Ag_2S/WS_2	Photocatalytic water oxidation and oxygen reduction reactions	Photodynamic/photothermal-synergistic therapy	61

synthetic MNRs. A typical example is the cell motors fabricated through macrophage uptake of functionalized magnetic NPs, by exploiting the engulfment capabilities of phagocytes.[29] It is an innovative strategy that combines the controlled navigation ability of synthetic NPs with the innate capabilities of immune cells. This will be helpful in improving the precision and efficiency of cancer treatment. However, the clinical transformation of these micromotors is still facing challenges. The reliance on external magnetic fields for guidance necessitates specialized equipment and continuous medical imaging, which requires precise manipulation skills and may not be feasible in remote clinical settings. Additionally, the high cost of magnetic driving devices and the need for continuous monitoring further complicate the clinical transformation of these micromotors. Many magnetic materials, such as nickel-based and neodymium-based metals, have poor biocompatibility and may cause adverse reactions in the human body. Their long-term effects and potential toxicity still need thorough investigation. To overcome these limitations, Yue *et al.* have pioneered a novel self-propelled macrophage motor.[30] The micromotor is engineered by intracellularly assembling MnO_2 NPs through host–guest interactions. These NPs enable the propulsion of micromotors through the consumption of H_2O_2 to produce O_2, thus enhancing tissue infiltration. When loaded with anti-inflammatory drugs, these micromotors can rapidly target and infiltrate into the lung with inflammation, offering a promising strategy for acute pneumonia treatment.

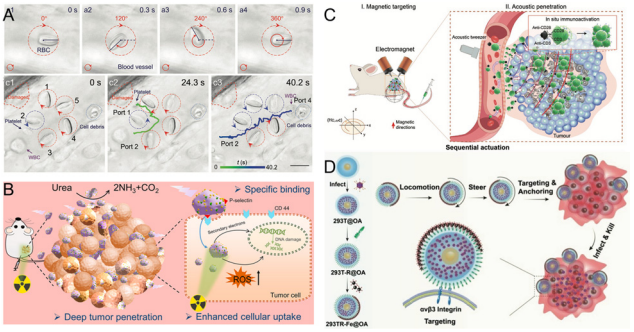

Fig. 2 LMNRs based on mammalian cells. (A) Living RBC microrouters for transporting platelets and WBCs. Reproduced with permission.[23] Copyright 2023, Wiley-VCH. (B) Urease propelled platelet cell motors for radiosensitization. Reproduced with permission.[26] Copyright 2023, Elsevier. (C) CAR T-cell based living microrobots for precise cancer immunotherapy. Reproduced with permission.[32] Copyright 2023, Wiley-VCH. (D) OA-loaded Janus cell robots for targeted virotherapy. Reproduced with permission.[33] Copyright 2022, Wiley-VCH.

The advent of immune cell-based MNRs marked a significant stride in cancer immunotherapy. In the field of advanced immunotherapy, adoptive T cell transfer (ACT) has emerged as a promising strategy. The recent approval of chimeric antigen receptor (CAR) T cell therapy by the Food and Drug Administration (FDA) has revolutionized the traditional treatments for patients with refractory pre-B cell acute lymphoblastic leukemia and diffuse large B cell lymphoma.[31] However, the application of CAR T-cell therapy in solid tumors remains challenging due to formidable physical barriers and a highly immunosuppressive microenvironment within these tumors. To address this issue, Tang *et al.* introduced CAR T-cell-based living micromotors (M-CAR T), which integrated acoustic responsive immunomagnetic beads on the cell surface of CAR T cells through click conjugation (Fig. 2C).[32] These micromotors can be precisely guided by an external gradient magnetic field to accumulate at the peritumoral margins of solid tumors. Immune cell-based MNRs showed us exciting potential for tumor therapy. We think more and more applications will appear in this area.

2.4. Cancer cells

Cancer cells exhibit remarkable abilities to survive and proliferate in the microenvironments of the body. They are capable of invading adjacent tissues and metastasizing to distant sites *via* the bloodstream or lymphatic systems. In light of this, Cong *et al.* have engineered a kind of cancer cellular robot as an active carrier of oncolytic adenoviruses (OA), acting as a "Trojan Horse" to target tumors (Fig. 2D).[33] These cellular robots are prepared by modifying OA-infected 293T cells and asymmetrically attaching Fe_3O4 NPs to the cell surface, endowing them with effective motility under magnetic control.

2.5. Sperm cells

Sperm cell-driven microrobots, or spermbots, utilize flagella to propel in fluid environments. Spermbots are constructed by integrating sperm cells with different microstructures (such as tubular and helical structures) that are composited with titanium, iron, or polymers.[34] Advanced fabrication techniques including 3D printing, rolled-up nanotechnology, and lithography can be used to precisely fabricate these structures.[35] Additionally, magnetic navigation can be realized by incorporating sperm cells with magnetic nanoparticles.[36] Spermbots have shown immense potential in targeted drug delivery, cancer therapy, and assisted fertilization.[37] For instance, ZIF-8-coated spermbots can protect sperm cells from oxidative damage and antisperm antibodies, ensuring stability and functionality during drug delivery.[38] In reproductive medicine, spermbots provide a non-invasive approach to overcome male infertility. By guiding spermbots to the egg using magnetic fields, the probability of fertilization can be enhanced without invasive procedures.[39]

3. LMNRs based on plants

Plant cells or tissues possess many distinctive features that make them ideal for biomedicine and environmental protection, such as high biocompatibility, low immunogenicity, various functionalities, and easy availability. By arming plant cells with nanotechnologies, plant-hybrid MNRs open new avenues for precise drug delivery, combined therapy, and environmental remediation. Table 2 presents an overview of some representative studies in recent years in this field. It illustrated the types, propulsion mechanisms, compositions, and application fields of plant-based micro/nanorobots.

3.1 Pollen

Pollen-based micro/nanorobots (Pollenbots) have seen increasing applications in environmental remediation and biomedicine in recent years. The use of pollen particles as ideal carriers for the fabrication of Pollenbots can be attributed to properties such as their natural origin, biodegradability, porosity, and biocompatibility. A series of studies, recently, have utilized plant pollen particles as carriers by various ways of modification. In this section, we primarily concentrated on lotus and sunflower Pollenbots, as the two pollen types are commonly used as microrobot carriers. The development of pine and chrysanthemum Pollenbots was only briefly introduced. In addition, we presented a therapeutic microrobotic platform based on pollen typhae, which possess natural medicinal properties rooted in traditional Chinese herbal medicine.

Lotus Pollenbots are a class of self-propelled micro-devices prepared based on lotus pollen templates. These devices were known for their highly selective recognition and functions for organic pollutant degradation or environmental response. For example, Han *et al.* have developed ion-imprinted Janus magnetic lotus Pollenbots, a solution for the selective recognition and capture of Pb(II) ions, thereby addressing the issue of heavy metal ion removal from water sources.[62] The functional materials used in these Pollenbots include $MnO_2/CoFe_2O_4$.

Table 2 Summary of LMNRs based on plants

Category	Size	Composition	Motion mechanism	Applications	Ref.
Lotus pollen	~30 μm	$CoFe_2O_4/MnO_2$/Pb-IIP-MMTs	Magnetic actuation, decomposition of H_2O_2 by catalase	Pb(II) ions removal	62
	~30 μm	Ag/Mg(Ni)Al-LDH	Decomposition of H_2O_2 by catalase	Congo red removal	63
	25 μm	HRP/PDA/Fe_3O_4	Magnetic actuation, decomposition of H_2O_2 by catalase	NIR-triggered degradation of organic pollutants	77
Sunflower pollen	~30 μm	Au/Co	Magnetic actuation	Cancer cell perforation	78
	~30 μm	Ni/Ti/DOX	Magnetic actuation	Intracellular drug delivery	66
	~30 μm	MLMD/Fe_3O_4	Magnetic actuation	Biofilm eradication	68
	~30 μm	PDA	Thermophoresis under near-infrared irradiation	Cell capture and release	67
Pine pollen	~50 μm	Fe_3O_4/DOX	Magnetic actuation	Targeted drug delivery	69
Chrysanthemum pollen	~20 μm	MNPs	Magnetic actuation	Cell perforation and tissue regeneration	70
Typhae pollen	20.3–20.8 μm	Fe_3O_4	Magnetic actuation	Acute gastric bleeding	79
Callus cell	~20 μm	Fe_3O_4/vitamin C	Magnetic actuation	Plant cell clones generation	80
	~20 μm	Fe_3O_4	Magnetic actuation	Pesticides removal	73
Bud	200–600 nm	CHI/vitamin C	Acoustic propulsion	Amyloid aggregates degradation	81
	50–100 μm	Fe_3O_4/CIP	Magnetic actuation	Antibiotic delivery	75
Thylakoid	300 nm	PEG_{44}-b-PS_{160}	Oxygen bubble propulsion by water-splitting	—	76

Yang *et al.* introduced a distinct variant of lotus Pollenbots, named Ag/Mg(Ni)Al-LDH Janus micromotors (Fig. 3A).[63] By virtue of the lotus pollen template, these microrobots exhibited special 3D porous structures prepared through heat treatment, hydrothermal synthesis, and vacuum evaporation. The sporopollenin-exine-capsule (SEC) micromotors demonstrated significant efficiency in pollutant degradation. As shown in Fig. 3B, the PDA-coated SEC micromotors achieved a pollutant degradation efficiency of approximately 70% within 10 minutes under near-infrared (NIR) irradiation, compared to only 19.25% without NIR (Fig. 3B).[64]

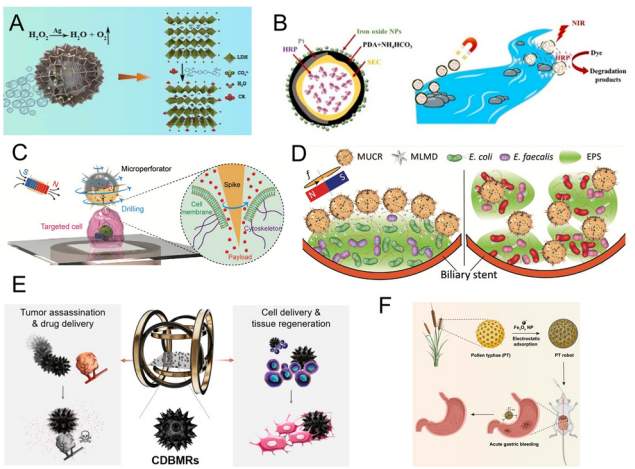

Fig. 3 Pollenbots. (A) Double hydroxide catalyzed lotus Pollenbots for organic pollutant removal. Reproduced with permission.[63] Copyright 2022, Springer Nature. (B) lotus Pollenbots for NIR triggered bioremediation of organic pollutants. Reproduced with permission.[64] Copyright 2021, Wiley-VCH. (C) Sunflower Pollenbots for single-cell perforation and targeted drug delivery. Reproduced with permission.[66] Copyright 2020, Wiley-VCH. (D) Magnetic urchin-like sunflower Pollenbots for biofilm eradication in biliary stents. Reproduced with permission.[68] Copyright 2022, Wiley-VCH. (E) Magnetic chrysanthemum Pollenbots for tumor assassination and active tissue regeneration. Reproduced with permission.[70] Copyright 2022, American Chemical Society. (F) Magnetic Typha Pollenbots for acute gastric bleeding treatment. Reproduced with permission.[71] Copyright 2022, American Chemical Society.

Sunflower Pollenbots are microrobots derived from pollen templates, offering another example of pollen hybrid microdevices. Inspired by the unique structure of sunflower pollen grains, these Pollenbots harness the natural nanospikes and internal cavity structure of pollen grains as a base carrier. By precisely modifying and functionalizing the surface and interior, they achieved accurate motion control and regulation in response to external stimuli. Sunflower Pollenbots exhibited various functionalities, such as drug delivery, anticancer, cell capture, and biofilm eradication. For instance, Mayorga-Martinez *et al.* have developed a kind of magnetically driven sunflower Pollenbot for capturing, manipulating, and killing cancer cells.[65] Under the influence of a rotating magnetic field, these Pollenbots can capture and transport cancer cells *via* electrostatic attraction. Besides, another kind of urchin-like sunflower Pollenbot with magnetic responsiveness was reported. Sun *et al.* fabricated these Pollenbots by removing the cytoplasm and surface lipids from sunflower pollen grains, preserving only the nanospike and cavity structures (Fig. 3C).[66] Under the influence of an external magnetic field, these Pollenbots can perforate tumor cells and release the chemotherapeutic DOX. Also, sunflower Pollenbots demonstrated potential for capturing, transporting, and releasing biological targets such as macromolecules or cells. Song *et al.* developed a sort of Pollenbot based on sunflower pollen grains that were modified with dopamine to endow them with photothermal conversion capability and special surface functionalization.[67] These Pollenbots used their spike-like structures and glycoprotein affinity to efficiently capture, transport, and release yeast cells. Capitalizing on the unique spike-like structure of sunflower pollen, Sun *et al.* developed a sunflower Pollenbot for eradicating bacteria in biliary stents (Fig. 3D).[68] Under the influence of the magnetic field, these Pollenbots used their

spike-like structure to penetrate the outer mucosal barrier of the biofilm and then release the magnetic liquid metal droplets, which worked as antimicrobial agents. From the above, by exploiting the unique properties of sunflower pollen, researchers have successfully designed and developed a diverse range of Pollenbots with varied functionalities, including drug delivery, cell capture, and biofilm eradication. We think sunflower Pollenbots have provided an efficient and effective approach for imaginative bio-applications or disease treatments in the future.

Recently, Pollenbots have also emerged as a promising platform for drug delivery. In the following sections, we discussed three additional types of pollen-based microrobots in this area: pine Pollenbots, chrysanthemum Pollenbots, and Typha Pollenbots. Pine Pollenbots were produced as bio-carriers, featuring the distinctive triple cavity structure, large air sacs, and porous outer walls. These characteristics provided excellent protection for drug payloads, while also ensuring uniformity, morphological stability, biocompatibility, autofluorescence, and physicochemical stability. Sun *et al.* encapsulated magnetic Fe_3O_4 nanoparticles and antitumor drugs, such as DOX, into the hollow cavities of pine pollen, providing the pine Pollenbots with advantages in motion control and drug release.[69] Thanks to their high maneuverability and controllability, pine Pollenbots can achieve precise treatment under complex physiological conditions. Chrysanthemum Pollenbots exhibited unique structural characteristics like hollow cavities, spike-like protrusions, and porous surface, which endowed them with high efficiency in drug and cell loading and release. In a recent study, Liu *et al.* loaded DOX into magnetic chrysanthemum Pollenbots by using vacuum infiltration technology (Fig. 3E).[70] Under the influence of a magnetic field, the Pollenbots were effectively tamed for physical killing and drug treatment against tumor cells. Furthermore, chrysanthemum Pollenbots also showed superior performance in active cell transport and tissue regeneration. Their porous surface structure and spike-like protrusions enhanced cell adhesion and tissue regeneration. The hollow cavity design enabled them to serve as cell carriers and transporters, ensuring cell viability and morphology during transport. In our opinion, chrysanthemum Pollenbots possess multiple functionalities, including targeted delivery, anchoring, killing, and drug release. We will see more interesting applications in various scenarios in the next few years. Typha Pollenbots, a newly emerged MNRs, were fabricated for treating acute gastric bleeding, inspired by a sort of traditional Chinese herbal medicine, Pollen Typhae. Taking advantage of the porous structure of Typha pollen microspheres, Yang *et al.* coated Fe_3O_4 nanoparticles onto the pollen surface to construct Typha Pollenbots (Fig. 3F).[71] Under the control of an external rotating magnetic field, Typha Pollenbots can precisely locate and treat bleeding sites within the body. In this case, we found an interesting point in Pollenbot design. In comparison to pine and chrysanthemum Pollenbots, Typha Pollenbots exhibited advantages in combining the curative effects of traditional Chinese medicine with microrobot technologies. These kinds of microrobots not only maintained the therapeutic efficacy of herbs but also possessed responsive and controllable functions. It may be a new approach for researchers to design innovative medical MNRs.

In conclusion, Pollenbots offer a promising and versatile platform for a wide range of applications, such as environmental remediation, disease treatment, and tissue regeneration. Future research on Pollenbots will involve a wider variety of pollen particles to increase their diversity and adaptability, as well as expand their functional strategies and potential applications in biomedicine. Additionally, exploring Pollenbots derived from various medicinal plants can further expand potential therapeutic applications. By harnessing the diverse therapeutic properties of traditional herbs, Pollenbots are expected to be developed with an extensive range of functionalities, tailored to address specific diseases.

3.2. Callus

Callus-based micro/nanorobots (Callusbots) represent a novel type of microscale robot that fuses plant callus tissue with functional micro/nanomaterials, offering promising capabilities for drug delivery and environmental remediation. Mayorga-Martinez *et al.* have successfully induced callus tissue from tomato leaf segments and co-cultivated them with magnetic Fe_3O_4 nanoparticles, resulting in tomato Callusbots with magnetic guidance. Propelled and guided by a rotating magnetic field, vitamin C attached to the Callusbots can be delivered to plant cells, in order to improve the growth of plant cells and protect them from oxidative stress damage (Fig. 4A).[72] Another example of tomato Callusbots took advantage of the inherent ability of callus cells to absorb and degrade organic compounds in water. Equipped with Fe_3O_4 nanoparticles, these Callusbots can rapidly and effectively remove the neurotoxic agent chlorpyrifos from water resources (Fig. 4B).[73]

In the field of environmental bioremediation, plant-based LMNRs offer advantages over synthetic nanomaterials due to the use of natural materials, like pollen and plant cells. These components are biodegradable, non-toxic, and biocompatible, which significantly reduces the risks associated with using

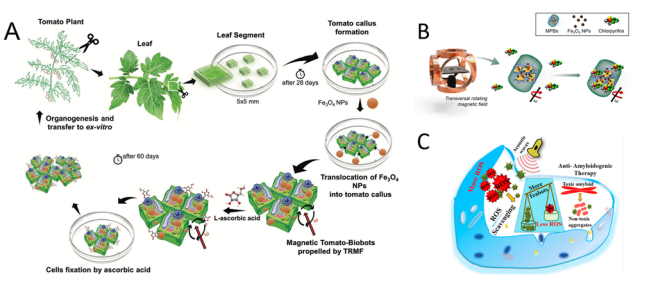

Fig. 4 Callusbots and Budbots. (A) Tomato-cell-based magnetic callus cellbots for the generation of plant cell clones. Reproduced with permission.[72] Copyright 2022, Wiley-VCH. (B) Tomato-cell-based magnetic callus cellbots for removing chlorpyrifos. Reproduced with permission.[73] Copyright 2022, Springer Nature. (C) Acoustic tea-Budbots for scavenging ROS and anti-amyloidogenic therapy. Reproduced with permission.[74] Copyright 2019, American Chemical Society.

LMNRs in ecosystems. Existing studies indicated that LMNRs were effective in degrading pollutants without showing significant ecological risks. However, to ensure environmental safety, future research should include localized ecological assessments before large-scale deployment. Such precautions will help confirm that LMNRs can aid in environmental remediation without harming ecosystem stability.

3.3. Buds

Buds of plants have also been employed, in recent research studies, to construct bud-based micro/nanorobots (Budbots). Bhuyan *et al.* disclosed tea-Budbots in two studies that aimed at ROS scavenging and bacterial biofilm removal, respectively. In one study, the tea-Budbots were fabricated by loading vitamin C onto the surface of nanoscale tea bud particles through electrostatic adsorption (Fig. 4C).[74] Under an ultrasound field, the tea-Budbots can scavenge oxidative stress induced ROS effectively. In another study, tea-Budbots were utilized for bacterial biofilm removal.[75] By modifying the tea buds of *Camellia sinensis* with magnetic Fe_3O_4 nanoparticles and chitosan, the tea-Budbots can electrostatically adsorb the antibiotic ciprofloxacin and release it in the acidic environment of the biofilm, achieving their antimicrobial effects. Similar to Typha Pollenbots, natural products were also employed in tea-Budbots to enhance the therapeutic effect. At this point, we think Budbots can play important roles in other areas such as anti-inflammatory, anti-tumor, and cardiovascular diseases in the future.

3.4. Thylakoids

Photosynthesis is a natural process in which light energy is harnessed to split water into oxygen and electrons, primarily catalyzed by Photosystem II (PS II) in thylakoid membranes within plant cells. Thylakoid-based micro/nanorobots (Thybots) are a kind of MNR constructed by using thylakoids extracted from plant cells. Mathesh *et al.* constructed Thybots by using the thylakoid extracted from spinach.[76] The propulsion of Thybots was governed by the combined action of oxygen bubbles produced by photosynthesis and the photophoresis effect. Thybots' motion can be controlled in real time by adjusting light intensity and direction. Current research primarily focuses on developing propulsion mechanisms; however, optimizing the design and exploring vesicles with different shapes, sizes, and opening dimensions are critical for advancing their potential applications, such as drug delivery, environmental remediation, and phototherapy.

4. LMNRs based on microorganisms

Besides using metazoan and plant cells in LMNRs, some researchers have also explored the use of microorganisms as power sources or functional components. Microorganisms have the characteristics of autonomous movement, rapid reproduction, easy manipulation, and modification, which make them ideal candidates for manufacturing LMNRs. Currently, various types of microorganisms have been used for the design and preparation of biohybrid micro/nanorobots, including microalgae, bacteria, yeast, *etc*. These microorganisms can be combined with therapeutic molecules, enzymes, metals, nanoparticles, and other components to form biohybrid micro/nanorobots with multiple functions and applications, such as enhancing photodynamic therapy, targeted cancer immunotherapy, gastrointestinal drug delivery, *etc*. Table 3 summarizes some representative studies on biohybrid micro/nanorobots based on microorganisms in recent years, including their types, compositions, propulsion mechanisms, and applications.

4.1. Microalgae

4.1.1. *Chlamydomonas*. *Chlamydomonas*-hybrid micro/nanorobots (Chlamydobots) represent a novel class of algae hybrid biorobots with potential in various biomedical applications. With the natural characteristics of motility, Chlamydobots show advantages in autonomous movement and phototactic capabilities. By engineering *Chlamydomonas*, researchers have developed various Chlamydobots with different functionalities.

One application of Chlamydobots was in the targeted delivery of chemotherapeutic drugs for tumor treatment. Akolpoglu *et al.* have successfully developed Chlamydobots capable of carrying the chemotherapeutic drug DOX (Fig. 5A).[82] They achieved this by coating the cell walls of *Chlamydomonas* with nanoparticles and using photocleavable linkers to bind DOX with the nanoparticles. This design strategy took advantage of the microalgae's phototactic and autonomous movement capabilities, improving drug targeting and reducing side effects. Moreover, Choi *et al.* used Chlamydobots to accelerate diabetic wound healing (Fig. 5B).[83] These Chlamydobots were functionalized with chitosan–heparin composites to enable deep oxygen delivery and removal of inflammatory chemokines. In the healing process of chronic wounds induced by diabetes, the Chlamydobots can penetrate blood clots and reach the depth of the wound by utilizing their autonomous movement and propulsion. Shchelik *et al.* have also studied antibiotic-conjugated Chlamydobots for drug delivery.[84] In one of the studies, Shchelik *et al.* attached the antibiotic vancomycin to the Chlamydobot surface *via* a self-cleaving disulfide linker (Fig. 5C).[85] This drug delivery system enabled targeted delivery and exhibited antimicrobial activities against Gram-positive bacteria. Similarly, Zhang *et al.* formed a self-propelling, fluorescent, phototactic, and long-lived Chlamydobot for treating lung infections by connecting antibiotic ciprofloxacin-loaded nanoparticles to microalgae *via* click chemistry.[86] Here, the *Chlamydomonas* served as carriers, relying on the self-propelled movement produced by their flagella. The phototactic ability of these microalgae allowed them to control and regulate for the precise treatment of acute bacterial pneumonia. Antibiotic-conjugated Chlamydobots enabled selected antibiotics to be attached to microalgae, offering a more targeted selection for treating specific types of bacterial infections. To enhance the tolerance of Chlamydobots in acidic environments and

Table 3 Summary of LMNRs based on microorganism

Category	Size	Composition	Motion mechanism	Applications	Ref.
Chlamydomonas	~10 μm	SIONPs/DOX	Flagellar propulsion	Light-triggered anticancer drug delivery	82
	~10 μm	CHI/Hep	Flagellar propulsion	Active oxygen delivery and immune modulation	83
	~10 μm	VAN or CIP	Flagellar propulsion	Antibiotic delivery	84
	~10 μm	VAN	Flagellar propulsion	Antibiotic delivery	85
	~10 μm	CIP		Acute bacterial pneumonia	86
	—	Enteric capsule	Flagellar propulsion	Gastrointestinal delivery	87
	~10 μm	*Chlamydomonas pitschmannii*	Flagellar propulsion	Gastrointestinal delivery	88
	~10 μm	ACE2 receptor	Flagellar propulsion	SARS-CoV-2 virus removal	89
	~10 μm	ACE2 receptor membrane vesicles	Flagellar propulsion	SARS-CoV-2 virus removal	90
Spirulina	50–80 μm	Fe_3O_4/TiO_2	Magnetic actuation	RhB degradation	91
	~200 μm	Fe_3O_4	Magnetic actuation	Cargo delivery	92
	25–35 μm, 100–200 μm	CuS/Fe_3O_4	Magnetic actuation	Photothermal therapy	93
	—	Fe_3O_4	Magnetic actuation	Photothermal therapy and environmental remediation	94
	100–200 μm	Fe_3O_4	Magnetic actuation	Radiosensitization and tumor-targeted imaging	95
	—	Au	Thermophoresis under near-infrared irradiation	Radiosensitization and tumor photothermal therapy	96
	200–500 μm	AMF	—	Radioprotection	97
	~22 μm	$BaTiO_3/Fe_3O_4$	Magnetic actuation, acoustic propulsion	Differentiation of neural stem-like cells	98
	140 μm	$BaTiO_3/Fe_3O_4$	Magnetic actuation, acoustic propulsion	Neuronal regenerative therapy	99
Chlorella	2–4 μm	$BiOCl/Fe_3O_4$	Magnetic actuation	Environmental remediation	102
	—	Ce6/PFTBA	—	Photodynamic therapy and Immune activation	103
	2.1 ± 0.8 μm	Erythrocyte membrane	—	Radiosensitization and tumor photodynamic therapy	104
	2.6 μm	CaP	—	Radiosensitization and tumor photodynamic/photothermal-synergistic therapy	105
	6.0 ± 0.7 μm	Fe_3O_4	Magnetic actuation	NIR-triggered contraction of muscle cells	106
Volvox	~60 μm	$Ce6/PDA/Fe_3O_4$	Flagellar propulsion	Photodynamic/photothermal-synergistic therapy and tumor-targeted imaging	109
E. coli	~2 μm	Zn-doped Fe_3O_4	Magnetic actuation	Magnetothermal ablation and imaging-guided tumor therapy	110
	~2 μm	Tellurium nanorods	—	Tumor photothermal immunotherapy	147
	~2 μm	Magnetic nanoparticle/ICG/DOX	Magnetic actuation, flagellar propulsion	Tumor penetration and NIR-triggered drug release	111
	~1 μm	HSulf-1/Glycogen/DOX	Flagellar propulsion	Anticancer drug delivery	112
	~1 μm	MS/DOX	Flagellar propulsion	Anticancer drug delivery	113
	~2 μm	ZIF-8/DOX	Flagellar propulsion	Anticancer drug delivery in harsh environments	116
	~2 μm	ZIF-8/DOX/ICG	Flagellar propulsion	Tumor penetration and photodynamic/photothermal-synergistic therapy	117
	~2 μm	Fucoidan/PDA/uPA microtubule	Flagellar propulsion	Thrombolysis	114
	~2 μm	PIF6/PhyB	Flagellar propulsion	Far red light-triggered cargo release	115
	~2 μm	PDA/uPA/GOx/CAT bacterial ghost	Decomposition of H_2O_2 by catalase	Thrombolysis	119
	~2 μm	FU/ZOL/Au bacterial ghost	—	Tumor photothermal immunotherapy	118
	20 ± 5 μm	$Mg/Au/TiO_2/CHI$	Reaction between Mg and H_2O	Tumor disruption and immunostimulatory	120
Bifidobacterium	~2 μm	BSA/DOX	—	Anticancer drug delivery	121
	~2 μm	Ce6/anti-DR5 Ab	—	Photodynamic/sonodynamic-synergistic therapy	122
	~2 μm	ICG	—	Photodynamic therapy	123
	~2 μm	PFH	—	Tumor high-intensity focused ultrasound ablation	124
AMB-1	2.18 ± 0.43 μm	—	Magnetic actuation	Pesticides removal	125
	1.8 μm	Liposomes	Magnetic actuation	Tumor infiltration and active drug delivery	148
	~4 μm	—	Magnetic actuation	Magnetothermal ablation for neuroblastoma	146

Table 3 *(Contd.)*

Category	Size	Composition	Motion mechanism	Applications	Ref.
	4.25 ± 0.89 μm	Ce6	Magnetic actuation	Photodynamic therapy	145
Yeast	~5 μm	ZIF-67/Fe_3O_4	Magnetic actuation	Mycotoxin decontamination	129
	~5 μm	5-ASA/curcumin/GOx/CAT	Decomposition of H_2O_2 by catalase	Gastrointestinal inflammation therapy	130
	~5 μm	$CaCO_3$/curcumin	$CaCO_3$ reacts with stomach acid to produce CO_2	Gastritis and gastric motility recovery	131
	2.76 ± 0.14 mm	Fe_3O_4	CO_2 production in sugar fermentation	Enhance the beer fermentation process	132
	~5 μm	TiO_2/PPy	Electroosmotic flows	Cell Manipulation	133
Mushroom	40 to 200 μm	curcumin/Fe_3O_4	Magnetic actuation	Bacterial removal in contaminated water	134
	50–160 μm	Fe_3O_4	Magnetic actuation, decomposition of H_2O_2 by catalase	Anticancer drug delivery	135
Spore	6–10 μm	Fe_3O_4	Magnetic actuation	Environmental remediation	136
	6 to 9 μm	Fe_3O_4/CDs	Magnetic actuation	Detection of toxins secreted by Clostridium difficile	149

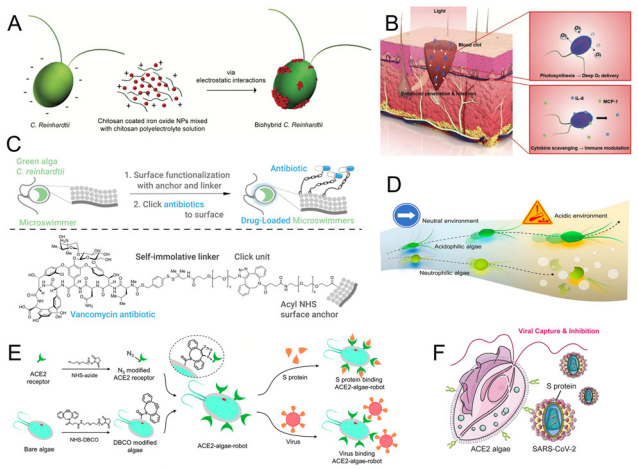

Fig. 5 Chlamydobots. (A) Chlamydobots loaded with Fe_3O_4 nanoparticles for drug delivery. Reproduced with permission.[82] Copyright 2020, Wiley-VCH. (B) Chlamydobots coated with chitosan–heparin nanocomplex for alleviating hypoxia and immune response in diabetic chronic wounds. Reproduced with permission.[83] Copyright 2022, Wiley-VCH. (C) Chlamydobots loaded with vancomycin for thiol-sensitive antibiotic drug release. Reproduced with permission.[85] Copyright 2023, Wiley-VCH. (D) *Chlamydomonas* embedded in a degradable capsule for intestinal drug delivery. Reproduced with permission.[88] Copyright 2022, AAAS. (E) ACE2 receptor-modified Chlamydobots for the removal of SARS-CoV-2 virus in wastewater. Reproduced with permission.[89] Copyright 2021, American Chemical Society. (F) Chlamydobots coated with ACE2 receptor-modified cell membrane vesicle for the removal of SARS-CoV-2 virus in wastewater. Reproduced with permission.[90] Copyright 2022, Elsevier.

improve their distribution and retention as gastrointestinal drug carriers, Zhang *et al.* designed Chlamydobots embedded in degradable capsules with an internal hydrophobic coating to protect *Chlamydomonas reinhardtii* from gastric acid erosion. Meanwhile, an external pH-sensitive coating was used to facilitate drug release in the intestinal environment.[87] In another research, Zhang *et al.* formed a type of acidophilic Chlamydobot by binding PLGA nanoparticles to the surface of *Chlamydomonas pitschmannii* (Fig. 5D).[88] This structure enabled effective self-propulsion and directed transport of the Chlamydobots in harsh acidic environments, allowing for drug delivery within the gastrointestinal tract. Lastly, Zhang *et al.* continued to create another kind of Chlamydobot, which was utilized in the clearance of the SARS-CoV-2 virus by modifying its surface with ACE2 receptors. They connected ACE2 receptors to the algae surface using click chemistry reactions, enabling the efficient capture of the virus (Fig. 5E).[89] Interestingly, a similar study was conducted by Lai *et al.* (Fig. 5F).[90]

In conclusion, Chlamydobots represent a promising class of microalgae hybrid biorobots, demonstrating a wide range of potential applications in the biomedical field. In addition to the applications mentioned above, such as cargo delivery, chronic wound healing, antibiotic release, and SARS-CoV-2 virus removal, there are numerous other possible areas yet to be explored. With the development of research, in our view, the versatilities and potentials of Chlamydobots in addressing diverse medical issues are expected to expand further.

4.1.2. Spirulina. Spirulina-hybrid micro/nanorobots (SP-bots) are micro/nanoscale machines derived from *Spirulina platensis*. By modifying the surface of spirulina with various functional materials, these SP-bots were utilized for environmental remediation, drug delivery, photothermal therapy, radiotherapy sensitization, and so on, as described below.

For environmental remediation, Mushtaq *et al.* have developed core–shell structured SP-bots using spirulina as the biotemplate and coating its surface with Fe_3O_4 and anatase-phase TiO_2.[91] These SP-bots demonstrated efficient degradation of organic dyes and other pollutants in water under ultraviolet-visible light or natural light. By combining multiple spirulina cells and coating their surface with Fe_3O_4 nanoparticles, Yan *et al.* endowed these SP-bots with magnetic and motion-controllable capabilities.[92] Such capabilities enabled them to navigate precisely in complex biological fluids, such as blood vessels or tissue microenvironments, delivering targeted molecular drugs with preserved biological activity to the desired location within the body. For photothermal therapy in cancer and antibacterial treatments, Gong *et al.* have developed

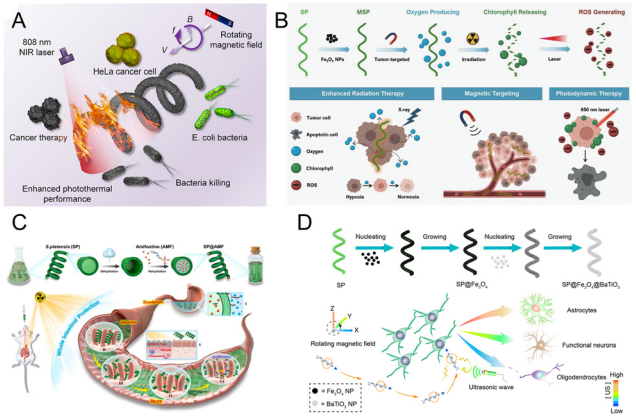

Fig. 6 SP-bots. (A) Spirulina-templated CuS/Fe_3O_4 SP-bots for enhanced photothermal performance in anticancer and antibacterial applications. Reproduced with permission.[93] Copyright 2021, Elsevier. (B) Magnetic SP-bots for tumor-targeted imaging and enhanced radiophotodynamic therapy. Reproduced with permission.[95] Copyright 2020, Wiley-VCH. (C) SP-bots carrying amifostine for intestinal protection in cancer radiotherapy. Reproduced with permission.[97] Copyright 2022, Springer Nature. (D) Magnetic SP-bots coated with piezoelectric $BaTiO_3$ nanoparticles for inducing neural stem cell differentiation and regeneration. Reproduced with permission.[99] Copyright 2021, American Chemical Society.

copper sulfide (CuS) nanoparticle-loaded SP-bots (Fig. 6A).[93] These SP-bots achieved efficient photothermal conversion and magnetic navigation by using CuS nanoparticles as photothermal agents and Fe_3O_4 nanoparticles as magnetic materials, with spirulina cells as carriers. Zheng *et al.* employed carbon and magnetite as functional materials for SP-bots, endowing them with the ability to kill bacteria and adsorb heavy metal ions.[94] These SP-bots exhibited various bio-functions, such as effective elimination of *E. coli* and adsorption of Cr^{6+} ions, in photothermal therapy. In the field of radiotherapy sensitization, Zhong *et al.* have engineered spirulina with photosynthesis capabilities to modulate the tumor microenvironment and enhance radiotherapy outcomes (Fig. 6B).[95] In another study, SP-bots with gold nanoparticles were used for dual-modal fluorescence and computed tomography (FL/CT) imaging-guided photothermal therapy in triple-negative breast cancer. Hosseini *et al.* utilized spirulina as a bio-template to regulate the distribution of gold nanoparticles and achieved tumor targeting through folic acid modification.[96] In the area of radiation protection, SP-bots have also been employed as an oral drug delivery system. Zhang *et al.* used spirulina as carriers to load amifostine into spirulina cells, creating a kind of specific SP-bot (Fig. 6C).[97] As for neural stem cell differentiation, Liu *et al.* have developed a minimally invasive, controllable system using biohybrid piezoelectrical magnetite SP-bots to induce neural stem cells to differentiate into specific types of functional neurons. This application provided new ideas for the treatment of neural injuries and neurodegenerative diseases.[98] In addition, under ultrasonic stimulation, SP-bots can generate different levels of local electric output by adjusting the intensity of ultrasound, thereby inducing neural stem cells to differentiate into various cell types, such as astrocytes, functional neurons (dopaminergic neurons, cholinergic neurons), and oligodendrocytes (Fig. 6D).[99] These SP-bots offered a potential approach for the treatment of neurodegenerative diseases. Another example is the application of spirulina-derived microrobots for imaging-guided therapy. By virtue of the intrinsic fluorescence of spirulina, microrobots in superficial tissues can be tracked *via* fluorescence.[100] However, the poor tissue penetration of fluorescence restricts its effectiveness for deep organ imaging. Instead, superparamagnetic nanoparticles with magnetic resonance imaging capabilities were integrated with spirulina because magnetic resonance imaging offers better tissue penetration and high spatial resolution.[101] Other medical imaging techniques such as ultrasound, radionuclide, and photoacoustic imaging can be also utilized to provide local information on LMNRs.

In summary, SP-bots have demonstrated significant potential in various applications, such as environmental remediation, drug delivery, photothermal therapy, radiation therapy enhancement, radiation protection, and neural stem cell differentiation. By using spirulina as a bio-template and modifying its surface with various functional materials, we reckon these SP-bots can be armed for more specific tasks, providing innovative solutions for diverse challenges in biomedicine and disease treatment.

4.1.3. *Chlorella*. *Chlorella*-hybrid micro/nanorobots (Chlobots) are a type of engineered microalgae that have been modified using bio-hybrid technologies, which enabled Chlobots with various functions. These functions included environmental remediation, cancer therapy, cancer sensitization, and activation of skeletal muscle cells. Herein, we offer a detailed review of these functionalities. In the field of environmental remediation, Chlobots have been designed with photocatalytic and magnetic capabilities by sequentially depositing Fe_3O_4 nanoparticles and BiOCl nanosheets on their surfaces. Under visible light, these Chlobots can efficiently degrade the organic dye rhodamine B and inactivate *Escherichia coli*, demonstrating significant potential for wastewater remediation.[102] For photodynamic therapy, Wang *et al.* have used Chlobots as carriers of photosensitizers and oxygen sources, thereby enhancing both local and systemic therapeutic effects as well as anti-tumor immune memory.[103] Concerning radiotherapy and photodynamic therapy sensitization, Qiao *et al.* used RBC membrane-coated *Chlorella* as a bioreactor that reduced the risk of macrophage phagocytosis and blood clearance, thus extending the circulation time of Chlobots within the body (Fig. 7A).[104] Under light exposure, *Chlorella* produces oxygen and ROS through photosynthesis, effectively improving the efficacy of radiotherapy and photodynamic therapy. In another study, Zhong *et al.* developed Chlobots by coating their surfaces with a protective layer of calcium phosphate (CaP).[105] Fluorescence and photoacoustic dual-mode imaging techniques were employed to monitor the real-time distribution and therapeutic effects of these microbots *in vivo*. In the field of skeletal muscle stimulation, magnetic Fe_3O_4 nanoparticles were coated on *Chlorella*'s surface.

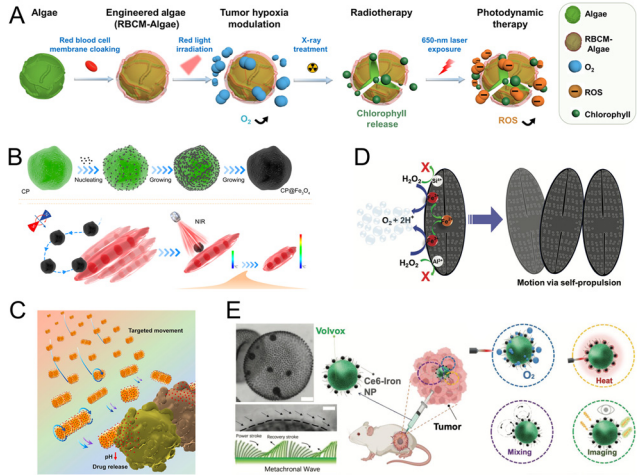

Fig. 7 Chlobots, Diatombots, and Volbots. (A) RBCM coated Chlobots for modulating tumor hypoxia and realizing cascade radio-phototherapy. Reproduced with permission.[104] Copyright 2020, AAAS. (B) Magnetic Chlobots for precise photothermal muscle activation. Reproduced with permission.[106] Copyright 2022, American Chemical Society. (C) Diatombots based on magnetic frustules for targeted drug delivery. Reproduced with permission.[107] Copyright 2022, Elsevier. (D) Iron oxide-embedded porous Diatombots. Reproduced with permission.[108] Copyright 2018, Royal Society of Chemistry. (E) Magnetic Volbots for precision imaging and photodynamic/photothermal synergistic therapy. Reproduced with permission.[109] Copyright 2022, Wiley-VCH.

Under the influence of magnetic fields and NIR lasers, these Chlobots were easy to control, effectively inducing the contraction of skeletal muscle cells in response to localized temperature increases (Fig. 7B).[106] In this case, we think it offered a non-invasive, precise, and biocompatible method for skeletal muscle tissue engineering.

4.1.4. Diatom. Mesoporous silica nanoparticles (MSNs) have emerged as a popular tool for biomedicine use, particularly in targeted drug delivery, attracting widespread attention from researchers. However, the use of MSNs was hindered by issues related to synthesis, such as complex procedures, time-consuming processes, and the involvement of toxic chemicals. In contrast, biomineralized porous silica shells known as frustules, produced by unicellular photosynthetic algae called diatoms, offer a natural alternative to MSNs. Found in nature, these frustules possess intricate 3D structures and porous surfaces, laying the groundwork for Diatom-hybrid micro/nanorobot (Diatombot) research.

The surface features and porous structure of diatoms make them suitable for drug loading. Li *et al.* obtained frustules capable of serving as drug carriers by treating diatoms with hydrochloric acid (Fig. 7C).[107] Subsequently, by loading doxorubicin (DOX) and attaching Fe_3O_4 magnetic nanoparticles to the diatom shell surface through electrostatic adsorption, the resulting magnetic Diatombots can deliver chemotherapeutic drugs to tumors. In another instance, researchers revealed that the frustules of magnetic Diatombots have a cylindrical structure, enabling them to roll along both their longitudinal and transverse axes under the same rotating magnetic field strength. Moreover, natural diatoms contain a trace amount of Fe_2O_3, which can be converted to Fe_3O_4 by cleaning with a NaOCl solution and then undergoing thermal decomposition treatment under an N_2 atmosphere. This process enhanced the diatoms' catalytic properties, allowing them to decompose H_2O_2 and generate propulsion (Fig. 7D).[108] Due to the asymmetric morphology of diatoms, the oxygen bubble force is anisotropic in solutions, enabling the Diatombots to move unidirectionally. To regulate Diatombot movement, in this study, EDTA was introduced as a chelating agent to block the catalytically active sites on the diatom surface, thereby playing the role of "braking". However, compared to MSNs, we deem Diatombots still face challenges in accurately controlling the size and shape of their frustules. Therefore, further exploration of a wider variety of diatom species and optimization of preparation is needed to better the design of the Diatombot.

4.1.5. *Volvox*. *Volvox* is composed of thousands of surface somatic cells organized in a hollow sphere, with each cell bearing two outward-pointing flagella. *Volvox*-hybrid micro/nanorobots (Volbot) were inspired by these multicellular green algae, *Volvox*. So far, Volbot has exhibited multimodal functionalities for precise imaging and treatment. Wang *et al.* explored the use of natural *Volvox* as carriers, combining them with photosensitizer-loaded chitosan and dopamine-functionalized magnetic nanoparticles through electrostatic adsorption to form a composite structure (Fig. 7E).[109] These Volbots can move along predetermined paths and directions under external magnetic fields, and generate oxygen to alleviate tumor hypoxia when exposed to light stimuli. In light of this design, these Volbot were apt to facilitate multimodal imaging, including fluorescence, photoacoustic, photothermal, and magnetic resonance imaging, for precise tumor detection and diagnosis. However, from our perspective, the relatively large size of the *Volvox* microalgae (approximately 50–60 μm) presented challenges for cargo delivery or penetration of deep solid tissues and organs. Consequently, it is crucial to investigate a suitable administration route and develop efficient drug delivery systems to overcome the limitations caused by the large size of the *Volvox* microalgae.

4.2. Bacterium

4.2.1. *Escherichia coli*. *Escherichia coli* is one of the most common bacteria closely related to our daily lives. *Escherichia coli*-hybrid micro/nanorobots (*E. coli*-Bacterbots) were modified to possess diverse functionalities and showed us great potential in various applications. Recent studies have reported *E. coli*-Bacterbots serving as carriers for drug delivery, magnetic hyperthermia, photothermal therapy, and immunotherapy, aiming to enhance the precision and effectiveness of treatments.

In the past few years, investigators developed diverse driving modes for *E. coli*-Bacterbots. Magnetic driving was used widely. Chen *et al.* designed *E. coli*-Bacterbots with magnetic thermal, hypoxic, and spatial magnetic sensing capabilities (Fig. 8A).[110] In this system, *E. coli* functioned as biological

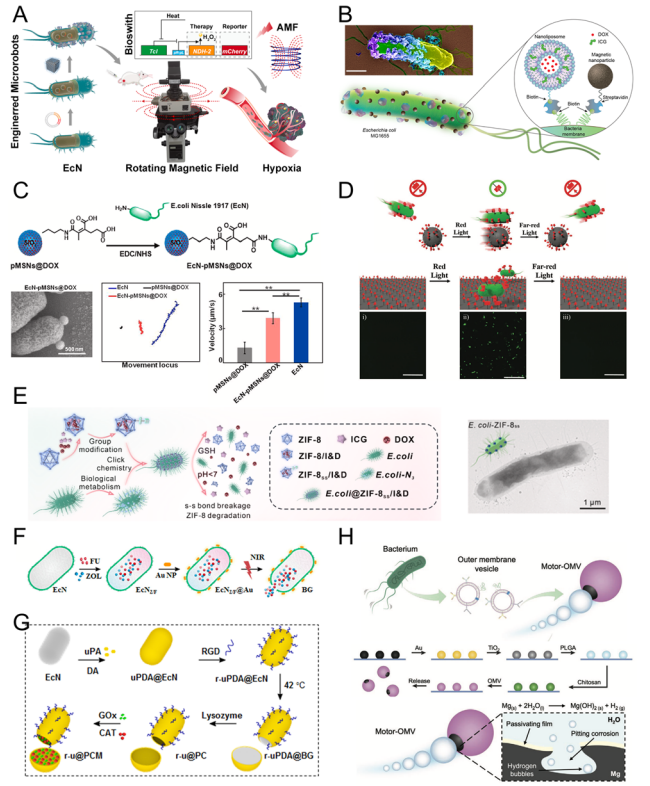

Fig. 8 *E. coli*-bacterbots. (A) Magnetic *E. coli*-bacterbots for magnetothermal bioswitched cancer therapy and imaging monitoring. Reproduced with permission.[110] Copyright 2022, American Chemical Society. (B) Magnetic *E. coli*-bacterbots carrying DOX and ICG-loaded nanoliposomes for cargo delivery. Reproduced with permission.[111] Copyright 2022, AAAS. (C) *E. coli*-bacterbots binding of pH-sensitive mesoporous silica nanocarriers for hypoxia targeted intestinal tumor therapy. Reproduced with permission.[113] Copyright 2023, Elsevier. (D) PhyB-PIF6 mediated red/far-red light switchable *E. coli*-bacterbots for targeted cargo delivery. Reproduced with permission.[115] Copyright 2019, Wiley-VCH. (E) MOF coated *E. coli*-bacterbots for tumor microenvironment-responsive deep drug delivery and photodynamic/photothermal therapy. Reproduced with permission.[117] Copyright 2022, Elsevier. (F) Gold nanorod-decorated bacterial ghost for targeted drug delivery and photothermal immunotherapy. Reproduced with permission.[118] Copyright 2021, Elsevier. (G) PDA coated *E. coli*-bacterbots based on GOx/CAT-driven bacterial ghost for uPA/RGD-mediated thermo-responsive thrombolysis. Reproduced with permission.[119] Copyright 2022, American Chemical Society. (H) *E. coli*-bacterbots for physical disruption of tumor tissue and immunostimulatory therapy. Reproduced with permission.[120] Copyright 2021, Wiley-VCH.

carriers and were controlled magnetically by packing magnetic nanoparticles into *E. coli*-Bacterbots. Furthermore, *E. coli*-Bacterbots have also shown potential in drug delivery. In another study on magnetically-driven *E. coli*-Bacterbots, Akolpoglu *et al.* employed magnetic nanoparticles and liposomes as carriers and functional materials (Fig. 8B).[111] These magnetically-driven *E. coli*-Bacterbots demonstrated precision and controllability in drug delivery and release, providing new strategies for cancer treatment. Apart from magnetically controlled *E. coli*-Bacterbots, chemotaxis of *E. coli* can also be utilized for drug delivery.[112] For instance, Wang *et al.* used *E. coli*-Bacterbots to transport drug-loaded mesoporous silica nanoparticles into intestinal tumors (Fig. 8C).[113] These *E. coli*-Bacterbots can improve drug penetration and cellular uptake in acidic environments, subsequently inhibiting tumor growth and inducing tumor cell apoptosis. Except for magnetic and chemotaxis driving, *E. coli*-Bacterbots can be designed to be driven or controlled by light, such as $^{Fu}PDA_{uPA}$@EcN microtubule Bacterbots[114] and red/far-red light-controllable Bacterbots (Fig. 8D).[115]

Improving the structural design of *E. coli*-Bacterbots is crucial. Recent studies have introduced various carriers and functional materials that enhance the structural design of *E. coli*-Bacterbots. To protect the physiological activity of *E. coli*, metal–organic frameworks (MOFs) have been used as functional materials, encapsulating the bacteria and providing cellular protection and active drug delivery. Li *et al.* utilized ZIF-8 as a functional material in metal–organic framework-based *E. coli*-Bacterbots.[116] In these Bacterbots, the ZIF-8 shell effectively prevents external enzyme intrusion, maintaining bacterial morphology, activity, and motility. In another instance, Zeng *et al.* employed a metal–organic framework that can dissociate in the tumor microenvironment in response to reducing agents and acidic conditions to construct tumor-targeting *E. coli*-Bacterbots (Fig. 8E).[117] In these Bacterbots, MOF nanoparticles on the bacterial surface degraded in the tumor microenvironment, releasing drugs and photosensitizers for combined tumor therapy, exhibiting significant advantages in treatment efficiency and anti-tumor effects. Besides MOFs, bacterial ghosts (BGs) were used as a new emerging strategy for *E. coli*-Bacterbots structure fabrication. These treated bacteria retained complete cell wall structures with large intracellular space and transmembrane tunnels for loading drugs or other substances. In addition, BGs can activate immune responses and induce macrophage polarization. Xie *et al.* loaded them with the chemotherapeutic drug 5-fluorouracil (FU) and macrophage phenotype modulator zoledronic acid (ZOL), and modified their surface with functional materials of gold nanorods (Au NRs) (Fig. 8F).[118] Moreover, Xie *et al.* found that *E. coli*-Bacterbots, with BGs as drug delivery carriers, could autonomously move in the bloodstream, effectively penetrating thrombi and releasing thrombolytic drugs (Fig. 8G).[119] These discoveries about BGs, in our thinking, could provide a new way of promoting thrombolysis, restoring blood flow, and reducing side effects in future clinical treatments. Except for BGs, bacterial outer membrane vesicles (OMVs) can also be found in recent *E. coli*-Bacterbot studies. For example, Zhou *et al.* have explored OMVs as immunostimulants to induce anti-tumor immune responses in their *E. coli*-Bacterbots research (Fig. 8H).[120]

In summary, the interesting elements, such as metal–organic frameworks, bacterial ghosts, and bacterial outer membrane vesicles, introduced in *E. coli*-Bacterbots nowadays provide the potential for *E. coli*-Bacterbots in various biomedical applications. These versatile Bacterbots have been employed for targeted drug delivery, photothermal therapy, immunotherapy, thrombolysis, and so on. Future research, in

our estimation, should continually focus on the optimization of the *E. coli*-Bacterbots' structure design and enhance their targeting capabilities. We hope more and more new biostructures and functional materials could be explored to expand *E. coli*-Bacterbots potential applications.

4.2.2. *Bifidobacterium*. As one of the current hotspots in bacterium based MNRs research, *Bifidobacterium*-hybrid micro/nanorobots (Bifido-Bacterbots) represent a promising biomedical delivery system, owing to the selective localization of *Bifidobacterium infantis* to hypoxic tumor environments. It provided Bifido-Bacterbots with potential applications for targeted diagnosis and treatment of tumors. By employing various fabrication strategies, Bifido-Bacterbots have been used to transport and release drugs or other therapeutic materials, enabling chemotherapy, photodynamic therapy, and photothermal therapy for tumor treatment.

In the application of chemotherapy, Xiao *et al.* developed a type of Bifido-Bacterbot that can deliver DOX to hypoxic tumor regions, with DOX wrapped in bovine serum albumin (BSA) then attached to the surface of Bifidobacteria (Fig. 9A).[121] The Bifido-Bacterbots inhibited tumor growth and metabolism through inducing tumor cell apoptosis. Bifido-Bacterbots can also be used for targeted phototherapy of tumors by loading them with photosensitizers or photothermal agents. For instance, Li *et al.* Synthesized Bifido-Bacterbots modified with anti-death receptor 5 antibodies and loaded with Ce6 photosensitizer nanoparticles.[122] Additionally, Reghu *et al.* carried out research on tumor photothermal therapy by encapsulating ICG in Cremophor EL nanoparticles, which were internalized by Bifidobacteria (Fig. 9B).[123] Bifido-Bacterbots can also be employed in other tumor treatment methods beyond chemotherapy and phototherapy. Chen *et al.* combined Bifidobacteria with perfluorohexane nanoparticles to enhance high-intensity focused ultrasound treatment with Bifido-Bacterbots.[124] This combination increased the thermal and mechanical effects of ultrasound, accelerating the progress of tumor necrosis.

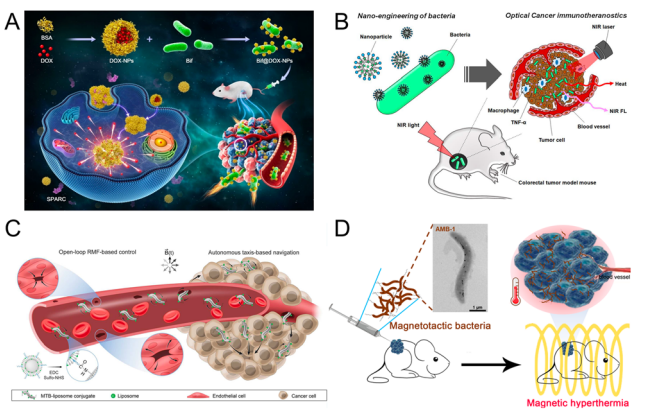

Fig. 9 Bifido-Bacterbots and AMB-1 Bacterbots. (A) Bifido-Bacterbots binding of DOX-loaded BSA nanoparticles for targeted chemotherapy in hypoxic tumor regions. Reproduced with permission.[121] Copyright 2022, Springer Nature. (B) Bifido-Bacterbots loaded with ICG for photothermal cancer immunotheranostics. Reproduced with permission.[123] Copyright 2022, American Chemical Society. (C) Magnetotactic AMB-1 Bacterbots for increased tumor infiltration. Reproduced with permission.[126] Copyright 2022, AAAS. (D) Magnetotactic AMB-1 Bacterbots mediated hyperthermia for neuroblastoma therapy. Reproduced with permission.[127] Copyright 2022, American Chemical Society.

As mentioned above, current research studies on Bifido-Bacterbots have explored the oxygen-deprived targeting ability of Bifidobacteria in hypoxic tumor environments in order to enhance tumor chemotherapy or photoacoustic therapy. We still think future studies should focus on optimizing the synthesis process of Bifido-Bacterbots and establishing more rational photoacoustic synergistic stimulation parameters, laying a solid foundation for clinical applications of Bifido-Bacterbots.

4.2.3. AMB-1. *Magnetospirillum magneticum* strain AMB-1 is a natural magnetotactic bacterium with helical morphology. The intrinsic properties of AMB-1 make it easy for autonomous self-propulsion or controlled maneuvering. It contains chains of magnetosomes composed of magnetic Fe_3O_4 nanoparticles. AMB-1 can be navigated under magnetic guidance, and their surfaces contain proteins that can bind to drugs or functional components. Recently, researchers have developed AMB-1 hybrid micro/nanorobots (AMB-1 Bacterbots) applied in environmental remediation and biomedicine.

For environmental remediation, Song *et al.* made a sort of AMB-1 Bacterbot for water decontamination, utilizing the natural adsorption effects of AMB-1.[125] Specifically, AMB-1 can function as biobot swarms, forming collective behavior through magnetic field manipulation, and effectively remove organophosphorus pesticides such as chlorpyrifos. In biomedicine application, AMB-1 can be employed as a drug carrier or therapeutic agent for targeted cancer treatment. Gwisai *et al.* constructed a kind of cancer-targeting therapeutic AMB-1 Bacterbot capable of autonomously sensing biochemical signals or carrying drugs by covalently coupling fluorescent liposomes to the surface of AMB-1 (Fig. 9C).[126] Moreover, AMB-1 Bacterbots, with natural magnetotaxis, allowed them to be navigated to the tumor cores for in-depth treatment. In light of this, Chen *et al.* created AMB-1 Bacterbots by utilizing the magnetotaxis properties of intact AMB-1 for tumor hyperthermia treatment (Fig. 9D).[127] In another study, Wang *et al.* also attempted to bind the photosensitizer Ce6 to the surface of AMB-1 Bacterbots for tumor photodynamic therapy.[128] Ce6-coated AMB-1 Bacterbots can emit red fluorescence and migrate towards the tumor area under magnetic field guidance. After laser irradiation, AMB-1 Bacterbots can generate a large amount of ROS to effectively kill cancer cells.

Despite existing studies demonstrating the value of AMB-1 Bacterbots in the environment and biomedicine field, we still think more research studies are needed to expand the variety of AMB-1 Bacterbots with different driving mechanisms and functions. Also, the synergistic effects with other therapeutic approaches should be explored, paving the way for broader applications of AMB-1 Bacterbots in disease treatment. Moreover, in-depth investigations of drug loading and release

capabilities of AMB-1 Bacterbots are required, as well as the evaluation of their safety and immune responses *in vivo*.

4.3. Fungus

While the potential of LMNRs based on microalgae and bacteria has been discussed, fungus-based LMNRs have not been thoroughly explored. Fungi possess various characteristics, including unique structures, metabolic pathways, and inherent biocompatibility, which make them promising candidates for the development of multifunctional and environmentally friendly robotic systems. Therefore, research into fungus-based LMNRs holds significant promise for applications in biomedicine and environmental remediation.

4.3.1. Yeasts. Yeast-hybrid micro/nanorobots (Yeast-bots) are bio-inspired micro/nanomachines that utilize yeast cells (*Saccharomyces cerevisiae*) as carriers or function elements. Yeast-bots can be used for various bio-functions with self-propelled movement. In recent years, significant research progress has been made in the application of Yeast-bots for fungal toxin removal, gastric inflammation treatment, and targeted therapy for inflammatory sites. To enhance the effectiveness of Yeast-bots, researchers have developed various fabrication methods and motion control technologies.

In a recent study, Lu *et al.* asymmetrically encapsulated Fe_3O_4 nanoparticles and metal–organic framework-67 (ZIF-67) on the surface of yeast cells to construct their Yeast-bots with fungal toxin removal capabilities.[129] For biomedical use, the twin-bioengine self-adaptive Yeast-bot system called TBY-robots has been developed for gastrointestinal inflammation treatments. To build these TBY-robots, Zhang *et al.* used yeast cell microcapsules as carriers and loaded them with anti-inflammatory drugs (Fig. 10A).[130] In another interesting research, Zhang *et al.* developed a special Yeast-bot with flower-like $CaCO_3$ crystals on the outer surface of yeast cells. In the acidic gastric environment, the external $CaCO_3$ reacted with H^+ ions, generating abundant CO_2 bubbles that drove the Yeast-bots through the gastric mucus layer and delivered drugs to treat gastric inflammation (Fig. 10B).[131] Taking advantage of yeast cells' metabolism, Maria-Hormigos *et al.* developed Yeast-bots with self-propelled movement through periodic bubble capture-release processes (Fig. 10C).[132] These Yeast-bots significantly accelerated the speed of beer fermentation. Furthermore, due to their magnetic accessories, these Yeast-bots can be separated from beer using magnetic fields. For investigation of driving modes, Wang *et al.* have designed a sort of Yeast-bot with an artificial cell wall based on TiO_2 nanoparticles.[133] Under ultraviolet light exposure, the Yeast-bots can decompose water to generate oxygen and hydrogen gases, propelling their motion.

Based on the above, it can be seen that the features of yeast cells' physiology and metabolism provide Yeast-bots with tremendous potential for use as carriers and functional materials. Researchers have successfully fabricated Yeast-bots using diverse preparation methods, such as magnetically driving, biocatalysis, and light-responsive control. These Yeast-bots will definitely offer new solutions in environmental remediation or disease therapy.

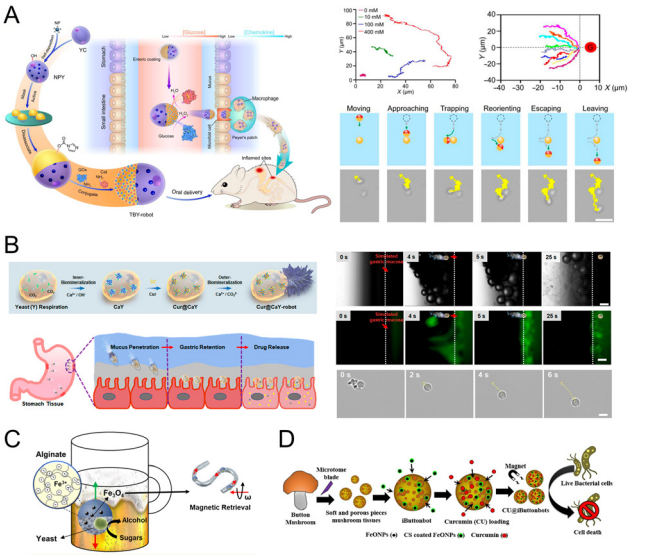

Fig. 10 Yeast-bots and Mushbots. (A) Schematic diagram of the fabrication of Yeast-bots and their application in active target delivery and GI inflammation therapy. Reproduced with permission.[130] Copyright 2023, AAAS. (B) Design of yeast-cell-based Cur@CaY-robot for penetration and gastritis therapy. Reproduced with permission.[131] Copyright 2023, American Chemical Society. (C) Alginate-encapsulated Yeast-bots for enhanced beer fermentation. Reproduced with permission.[132] Copyright 2023, American Chemical Society. (D) Magnetic Mushbots loaded with curcumin for the eradication of *E. coli* in water. Reproduced with permission.[135] Copyright 2020, Springer Nature.

4.3.2. Mushrooms. Edible mushrooms, specifically *Agaricus bisporus*, commonly known as white or button mushrooms, are not only nutritious and medicinal but are also enriched with catalytic enzymes and porous structures. These unique characteristics make them an ideal substrate for biorobotics. Applications of mushroom-hybrid micro/nanorobots (Mushbots) across various fields involve a multitude of preparation strategies. For example, curcumin-loaded magnetic Mushbots were used for the destruction of *E. coli* in contaminated water,[134] while chemotherapy drug-loaded Mushbots were employed for targeted cancer treatments (Fig. 10D).[135] Researchers utilized edible *Agaricus bisporus* as carriers, and combined it with magnetic Fe_3O_4 nanoparticles and other functional materials or drugs. Specific preparation methods involved mushroom slicing, drying, crushing, and coating, so as to form specific Mushbots that can address biomedical and environmental issues. Despite promising potential of the aforementioned applications, Mushbots also have their limitations. For example, the dimensions of Mushbots were relatively large (40–200 μm), which may affect their dispersion and penetration in water. Therefore, it is necessary to improve the quality of Mushbots and optimize their shape, size, and surface functionalization to adapt to various application requirements. Additionally, further investigations are still needed for intelligent control of the motion of the Mushbots in response to endogenous or exogenous stimuli, such as light, pH, or temperature.

4.3.3. Spores. Spores have complex 3D architectures with numerous active sites and specific surfaces due to their porosity. For example, *Ganoderma lucidum*, commonly known as "Lingzhi", a type of fungus from China, is renowned for its natural remedies. Its spores feature a natural porous, rough, and negatively charged microstructure. When modified, these multifunctional and highly potent Lingzhi spores can be utilized as templates for developing novel functional materials. Previous studies have successfully applied Lingzhi spore-hybrid micro/nanorobots (Lingzhi-Sporebots) in environmental remediation and toxin detection.[136]

5. Conclusions

In recent years, LMNRs, which can convert various forms of energy into spontaneous motion and navigation, have emerged as advanced micro- and nanoscale devices that are gaining attention in the field of biomedicine due to their significant potential. This paper reviewed several types of LMNRs and their diverse biomedical applications, which are based on different living materials or biological assemblies, including mammalian cells, plants, and microorganisms. In the realm of biomedical applications, LMNRs present an exciting prospect for future developments.

Compared to inorganic materials, "living" components offered advantages that allowed MNRs to explore new horizons. These advantages are outlined below. (1) Self-driving: Traditionally synthesized MNRs tended to be designed to be driven by an external magnetic field in many cases. However, the external force field was not always suitable or available, especially for MNRs delivered deep into human organs. This problem was absent in LMNRs due to the self-propelling power provided by living entities, such as LMNRs based on sperms[34,137] and *Chlamydomonas*.[138] (2) Bio-affinity: In general, inorganic materials have often been challenged by their lack of biocompatibility and ability to target specific sites *in vivo*. However, living materials integrated with these inorganic materials can facilitate the targeting of predetermined sites, such as diseased organs or tumors. For example, LMNRs that use cancer cell membranes as camouflage are being utilized for targeted cancer treatments.[139] (3) Less adverse effects: Unlike inorganic materials, living carriers in LMNRs, like RBCs, PLTs, and other cells, reduced the risk of heavy metal accumulation in the human body. Additionally, LMNRs were apt to involve simpler synthesis and environmentally friendly manufacturing processes.[140] These traits made LMNRs a more sustainable and innovative option in the field of next-generation nanotechnology.[141]

Recent advancements in developing LMNRs have brought forth new directions and trends. (1) One notable trend in research is the use of cell membranes. In addition to studying intact living organisms, such as cells and microorganisms, researchers have increasingly turned to incomplete organelles. Among these, cell membranes have become some of the most widely utilized. This approach leveraged the unique properties of these membranes, including their ability to evade the immune system and target specific cells or tissues. As a result, nanomotors can deliver therapeutic agents more efficiently and accurately. Various types of cell membranes have been reported in recent LMNR studies, including red blood cell membranes, platelet membranes, white blood cell membranes, cancer cell membranes, and bacterial outer membranes. (2) Another significant trend is the utilization of living carriers that possess their own therapeutic effects, such as Typhae pollen,[79] immune cells,[142] and stem cells.[143,144] Clearly, in addition to their roles as carriers, these cells also contributed their own healing properties to the medical applications of LMNRs. This approach opens up new possibilities for designing LMNRs using natural resources, particularly Chinese medicinal materials. (3) Additionally, bio-carriers with specialized functions are drawing attention in the field of LMNRs. Researchers are interested in finding or developing carriers that possess unique functionalities. A notable example is the *Magnetospirillum magneticum* strain AMB-1,[145,146] known for its natural magnetotactic properties, which has become popular in recent LMNR research. Furthermore, genetic engineering has been applied to increase the therapeutic potential of these carriers, such as programming bacteria to produce specific proteins that can inhibit carcinogenesis and angiogenesis.[112]

As we have seen, LMNRs have significant potential for application across various fields. However, their future development directions require further consideration. We believe that tumor treatment represents the most promising area for LMNRs' future applications. In cancer therapy, LMNRs function as effective vehicles for delivering anti-tumor drugs, viral vectors, immunomodulators, or nanoparticles to lymph nodes or mucosal surfaces. Due to their ability to combine with various elements, LMNRs can produce chemotherapeutic, photothermal, magnetothermal, and photodynamic effects that help to eliminate cancer cells. Compared to traditional passive systems, LMNRs offer remarkable advantages in disease treatment. However, challenges and limitations must be addressed before their translation into clinical practice. These include enhancing their biocompatibility, biodegradability, and biosecurity in living systems, as well as improving their bioefficacy, accuracy, and controllability in complex environments. Additionally, efforts should be made to expedite their feasibility, quality, and uniformity during mass production. Comprehensive research should also be conducted to evaluate their long-term effects, toxicity, clearance mechanisms, immunological responses, ethical issues, and regulatory standards. We hope this review illuminates the current status of LMNRs in biomedical applications and provides insight for further research in this emerging field.

Author contributions

Shuhuai Wang: conceptualization, writing – original draft, and visualization; Ya Liu: writing – review & editing; Shuangjiao Sun: writing – review & editing; Qinyi Gui: writing – review &

editing; Wei Liu: supervision, project administration, and funding acquisition; Wei Long: supervision, project administration, and funding acquisition.

Data availability

No primary research results, software or code have been included and no new data were generated or analysed as part of this review.

Conflicts of interest

The authors declare no conflict of interest.

Acknowledgements

This work was supported by the National Natural Science Foundation of China (No. 32401195), the Fundamental Research Funds for the Central Universities (3332023064) and the CAMS Innovation Fund for Medical Sciences (CIFMS, no. 2021-I2M-1-042).

References

1 S. Wang, X. Liu, Y. Wang, D. Xu, C. Liang, J. Guo and X. Ma, *Nanoscale*, 2019, **11**, 14099–14112.
2 T. Liu, L. Xie, C.-A. H. Price, J. Liu, Q. He and B. Kong, *Chem. Soc. Rev.*, 2022, **51**, 10083–10119.
3 D. Wang, A. Mukhtar, M. Humayun, K. Wu, Z. Du, S. Wang and Y. Zhang, *Chem. Rec.*, 2022, **22**, e202200016.
4 Y. Dong, L. Wang, V. Iacovacci, X. Wang, L. Zhang and B. J. Nelson, *Matter*, 2022, **5**, 77–109.
5 Y. Wang, Y. Tu and F. Peng, *Micromachines*, 2021, **12**, 222.
6 L. Ren, F. Soto, L. Huang and W. Wang, in *Field-Driven Micro and Nanorobots for Biology and Medicine*, ed. Y. Sun, X. Wang and J. Yu, Springer International Publishing, Cham, 2022, pp. 29–60.
7 J. Zhang, Z. Chen, R. K. Kankala, S.-B. Wang and A.-Z. Chen, *Int. J. Pharm.*, 2021, **596**, 120275.
8 Y. Zhang, Y. Zhang, Y. Han and X. Gong, *Micromachines*, 2022, **13**, 648.
9 F. Soto, J. Wang, R. Ahmed and U. Demirci, *Adv. Sci.*, 2020, **7**, 2002203.
10 Y. Guo, D. Jing, S. Liu and Q. Yuan, *Theranostics*, 2023, **13**, 2993–3020.
11 E. Rahimi, R. Sanchis-Gual, X. Chen, A. Imani, Y. Gonzalez-Garcia, E. Asselin, A. Mol, L. Fedrizzi, S. Pané and M. Lekka, *Adv. Funct. Mater.*, 2023, 2210345.
12 X. Chang, Y. Feng, B. Guo, D. Zhou and L. Li, *Nanoscale*, 2022, **14**, 219–238.
13 J. Ye, Y. Fan, Y. Kang, M. Ding, G. Niu, J. Yang, R. Li, X. Wu, P. Liu and X. Ji, *Adv. Funct. Mater.*, 2024, 2416265.
14 W. Xu, H. Qin, H. Tian, L. Liu, J. Gao, F. Peng and Y. Tu, *Appl. Mater. Today*, 2022, **27**, 101482.
15 H. Zhang, Z. Li and Q. He, *Adv. NanoBiomed Res.*, 2022, **2**, 2200094.
16 S. Shivalkar, P. Chowdhary, T. Afshan, S. Chaudhary, A. Roy, S. K. Samanta and A. K. Sahoo, *Colloids Surf., B*, 2023, **222**, 113054.
17 J. Li, H. Zhou, C. Liu, S. Zhang, R. Du, Y. Deng and X. Zou, *Aggregate*, 2023, e359.
18 B. Esteban-Fernández De Ávila, W. Gao, E. Karshalev, L. Zhang and J. Wang, *Acc. Chem. Res.*, 2018, **51**, 1901–1910.
19 J. Niu, C. Liu, X. Yang, W. Liang and Y. Wang, *Front. Bioeng. Biotechnol.*, 2023, **11**, 1277964.
20 Z. Wu, J. Li, B. E. De Ávila, T. Li, W. Gao, Q. He, L. Zhang and J. Wang, *Adv. Funct. Mater.*, 2015, **25**, 7497–7501.
21 Y. Zhu, H. Jia, Y. Jiang, Y. Guo, Q. Duan, K. Xu, B. Shan, X. Liu, X. Chen and F. Wu, *Exploration*, 2024, **4**, 20230105.
22 R. Gautam, Y. Xiang, J. Lamstein, Y. Liang, A. Bezryadina, G. Liang, T. Hansson, B. Wetzel, D. Preece, A. White, M. Silverman, S. Kazarian, J. Xu, R. Morandotti and Z. Chen, *Light: Sci. Appl.*, 2019, **8**, 31.
23 X. Liu, H. Wu, S. Wu, H. Qin, T. Zhang, Y. Lin, X. Zheng and B. Li, *Adv. Sci.*, 2023, **10**, 2304103.
24 T. Li, T. Chen, H. Chen, Q. Wang, Z. Liu, L. Fang, M. Wan, C. Mao and J. Shen, *Small*, 2021, **17**, 2104912.
25 S. Tang, F. Zhang, H. Gong, F. Wei, J. Zhuang, E. Karshalev, B. Esteban-Fernández de Ávila, C. Huang, Z. Zhou, Z. Li, L. Yin, H. Dong, R. H. Fang, X. Zhang, L. Zhang and J. Wang, *Sci. Rob.*, 2020, **5**, eaba6137.
26 W. Liu, H. Nie, H. Li, Y. Liu, M. Tian, S. Wang, Y. Yang and W. Long, *J. Colloid Interface Sci.*, 2024, **658**, 540–552.
27 X.-D. Zhang, D. Wu, X. Shen, J. Chen, Y.-M. Sun, P.-X. Liu and X.-J. Liang, *Biomaterials*, 2012, **33**, 6408–6419.
28 H. Pan, M. Zheng, A. Ma, L. Liu and L. Cai, *Adv. Mater.*, 2021, **33**, 2100241.
29 Y. Dai, L. Jia, L. Wang, H. Sun, Y. Ji, C. Wang, L. Song, S. Liang, D. Chen, Y. Feng, X. Bai, D. Zhang, F. Arai, H. Chen and L. Feng, *Small*, 2022, **18**, 2105414.
30 L. Yue, C. Gao, J. Li, H. Chen, S. M. Y. Lee, R. Luo and R. Wang, *Adv. Mater.*, 2023, 2211626.
31 C. H. June, R. S. O'Connor, O. U. Kawalekar, S. Ghassemi and M. C. Milone, *Science*, 2018, **359**, 1361–1365.
32 X. Tang, Y. Yang, M. Zheng, T. Yin, G. Huang, Z. Lai, B. Zhang, Z. Chen, T. Xu, T. Ma, H. Pan and L. Cai, *Adv. Mater.*, 2023, 2211509.
33 Z. Cong, S. Tang, L. Xie, M. Yang, Y. Li, D. Lu, J. Li, Q. Yang, Q. Chen, Z. Zhang, X. Zhang and S. Wu, *Adv. Mater.*, 2022, **34**, 2201042.
34 H. Xu, M. Medina-Sánchez and O. G. Schmidt, *Angew. Chem., Int. Ed.*, 2020, **59**, 15029–15037.
35 F. Rajabasadi, S. Moreno, K. Fichna, A. Aziz, D. Appelhans, O. G. Schmidt and M. Medina-Sánchez, *Adv. Mater.*, 2022, **34**, 2204257.
36 V. Magdanz, I. S. M. Khalil, J. Simmchen, G. P. Furtado, S. Mohanty, J. Gebauer, H. Xu, A. Klingner, A. Aziz,

M. Medina-Sánchez, O. G. Schmidt and S. Misra, *Sci. Adv.*, 2020, **6**, eaba5855.
37 A. Singh, M. Ansari, M. Mahajan, S. Srivastava, S. Kashyap, P. Dwivedi, V. Pandit and U. Katha, *Micromachines*, 2020, **11**, 448.
38 Q. Chen, S. Tang, Y. Li, Z. Cong, D. Lu, Q. Yang, X. Zhang and S. Wu, *ACS Appl. Mater. Interfaces*, 2021, **13**, 58382–58392.
39 V. Magdanz, M. Guix, F. Hebenstreit and O. G. Schmidt, *Adv. Mater.*, 2016, **28**, 4084–4089.
40 C. Gao, Z. Lin, D. Wang, Z. Wu, H. Xie and Q. He, *ACS Appl. Mater. Interfaces*, 2019, **11**, 23392–23400.
41 J. Shao, M. Abdelghani, G. Shen, S. Cao and D. S. Williams, *ACS Nano*, 2018, **12**, 4877–4885.
42 F. Zhang, J. Zhuang, B. Esteban Fernández de Ávila, S. Tang, Q. Zhang, R. H. Fang, L. Zhang and J. Wang, *ACS Nano*, 2019, **13**, 11996–12005.
43 X. Wei, M. Beltrán-Gastélum, E. Karshalev, B. Esteban-Fernández de Ávila, J. Zhou, D. Ran, P. Angsantikul, R. H. Fang, J. Wang and L. Zhang, *Nano Lett.*, 2019, **19**, 1914–1921.
44 B. Esteban-Fernández de Ávila, P. Angsantikul, D. E. Ramírez-Herrera, F. Soto, H. Teymourian, D. Dehaini, Y. Chen, L. Zhang and J. Wang, *Sci. Rob.*, 2018, **3**, eaat0485.
45 X. Pan, Q. Wang, S. Li, X. Wang and X. Han, *ChemistrySelect*, 2019, **4**, 10296–10298.
46 C. Gao, Z. Lin, C. Zhou, D. Wang and Q. He, *Chin. J. Chem.*, 2020, **38**, 1589–1594.
47 K. Hou, Y. Zhang, M. Bao, C. Xin, Z. Wei, G. Lin and Z. Wang, *ACS Appl. Mater. Interfaces*, 2022, **14**, 3825–3837.
48 M. Wan, Q. Wang, R. Wang, R. Wu, T. Li, D. Fang, Y. Huang, Y. Yu, L. Fang, X. Wang, Y. Zhang, Z. Miao, B. Zhao, F. Wang, C. Mao, Q. Jiang, X. Xu and D. Shi, *Sci. Adv.*, 2020, **6**, eaaz9014.
49 Y. Huang, T. Li, W. Gao, Q. Wang, X. Li, C. Mao, M. Zhou, M. Wan and J. Shen, *J. Mater. Chem. B*, 2020, **8**, 5765–5775.
50 J. Li, P. Angsantikul, W. Liu, B. Esteban-Fernández de Ávila, X. Chang, E. Sandraz, Y. Liang, S. Zhu, Y. Zhang, C. Chen, W. Gao, L. Zhang and J. Wang, *Adv. Mater.*, 2018, **30**, 1704800.
51 V. D. Nguyen, H.-K. Min, H. Y. Kim, J. Han, Y. H. Choi, C.-S. Kim, J.-O. Park and E. Choi, *ACS Nano*, 2021, **15**, 8492–8506.
52 V. Du Nguyen, V. H. Le, S. Zheng, J. Han and J.-O. Park, *J. Micro-Bio Robot.*, 2018, **14**, 69–77.
53 Y. Dai, X. Bai, L. Jia, H. Sun, Y. Feng, L. Wang, C. Zhang, Y. Chen, Y. Ji, D. Zhang, H. Chen and L. Feng, *Small*, 2021, **17**, 2103986.
54 F. Zhang, R. Mundaca-Uribe, H. Gong, B. Esteban-Fernández de Ávila, M. Beltrán–Gastélum, E. Karshalev, A. Nourhani, Y. Tong, B. Nguyen, M. Gallot, Y. Zhang, L. Zhang and J. Wang, *Adv. Mater.*, 2019, **31**, 1901828.
55 J. Wang, R. Ahmed, Y. Zeng, K. Fu, F. Soto, B. Sinclair, H. T. Soh and U. Demirci, *Small*, 2020, **16**, 2005185.
56 N. O. Dogan, H. Ceylan, E. Suadiye, D. Sheehan, A. Aydin, I. C. Yasa, A. Wild, G. Richter and M. Sitti, *Small*, 2022, **18**, 2204016.
57 H. X. Cao, V. D. Nguyen, D. Jung, E. Choi, C.-S. Kim, J.-O. Park and B. Kang, *Pharmaceutics*, 2022, **14**, 2143.
58 B. Huang, W. D. Abraham, Y. Zheng, S. C. Bustamante López, S. S. Luo and D. J. Irvine, *Sci. Transl. Med.*, 2015, **7**, 291ra94.
59 M. Zhou, Y. Xing, X. Li, X. Du, T. Xu and X. Zhang, *Small*, 2020, **16**, 2003834.
60 H. Zhang, Z. Li, Z. Wu and Q. He, *Adv. Ther.*, 2019, **2**, 1900096.
61 Y. Fu, F. Ye, X. Zhang, Y. He, X. Li, Y. Tang, J. Wang and D. Gao, *ACS Nano*, 2022, **16**, 18376–18389.
62 Y. Han, Y. Lyu, N. Xing, X. Zhang, K. Hu, H. Luo, D. H. L. Ng and J. Li, *J. Mater. Chem. C*, 2022, **10**, 15524–15531.
63 J. Yang, J. Li, P. Yang, N. Xing, Y. Chen, M. Zuo and T. Li, *J. Mater. Sci.*, 2022, **57**, 10953–10967.
64 S. Pan, J. Ren, E. Ma, K. Wang, S. Yang and H. Wang, *ChemNanoMat*, 2021, **7**, 483–487.
65 C. C. Mayorga-Martinez, M. Fojtů, J. Vyskočil, N. Cho and M. Pumera, *Adv. Funct. Mater.*, 2022, **32**, 2207272.
66 M. Sun, Q. Liu, X. Fan, Y. Wang, W. Chen, C. Tian, L. Sun and H. Xie, *Small*, 2020, **16**, 1906701.
67 L. Song, J. Cai, S. Zhang, B. Liu, Y.-D. Zhao and W. Chen, *Sens. Actuators, B*, 2022, **358**, 131523.
68 M. Sun, K. F. Chan, Z. Zhang, L. Wang, Q. Wang, S. Yang, S. M. Chan, P. W. Y. Chiu, J. J. Y. Sung and L. Zhang, *Adv. Mater.*, 2022, **34**, 2201888.
69 M. Sun, X. Fan, X. Meng, J. Song, W. Chen, L. Sun and H. Xie, *Nanoscale*, 2019, **11**, 18382–18392.
70 D. Liu, T. Zhang, Y. Guo, Y. Liao, Z. Wu, H. Jiang and Y. Lu, *ACS Appl. Bio Mater.*, 2022, **5**, 5933–5942.
71 Q. Yang, S. Tang, D. Lu, Y. Li, F. Wan, J. Li, Q. Chen, Z. Cong, X. Zhang and S. Wu, *ACS Appl. Bio Mater.*, 2022, **5**, 4425–4434.
72 D. Huska, C. C. Mayorga-Martinez, R. Zelinka and M. Pumera, *Small*, 2022, **18**, 2200208.
73 S.-J. Song, C. C. Mayorga-Martinez, D. Huska and M. Pumera, *NPG Asia Mater.*, 2022, **14**, 79.
74 T. Bhuyan, D. Dutta, M. Bhattacharjee, A. K. Singh, S. S. Ghosh and D. Bandyopadhyay, *ACS Appl. Bio Mater.*, 2019, **2**, 4571–4582.
75 T. Bhuyan, A. T. Simon, S. Maity, A. K. Singh, S. S. Ghosh and D. Bandyopadhyay, *ACS Appl. Mater. Interfaces*, 2020, **12**, 43352–43364.
76 M. Mathesh and D. A. Wilson, *Adv. Intell. Syst.*, 2020, **2**, 2000028.
77 S. Pan, J. Ren, E. Ma, K. Wang, S. Yang and H. Wang, *ChemNanoMat*, 2021, **7**, 483–487.
78 C. C. Mayorga-Martinez, M. Fojtů, J. Vyskočil, N. Cho and M. Pumera, *Adv. Funct. Mater.*, 2022, **32**, 2207272.
79 Q. Yang, S. Tang, D. Lu, Y. Li, F. Wan, J. Li, Q. Chen, Z. Cong, X. Zhang and S. Wu, *ACS Appl. Bio Mater.*, 2022, **5**, 4425–4434.

80 D. Huska, C. C. Mayorga-Martinez, R. Zelinka and M. Pumera, *Small*, 2022, **18**, 2200208.
81 T. Bhuyan, D. Dutta, M. Bhattacharjee, A. K. Singh, S. S. Ghosh and D. Bandyopadhyay, *ACS Appl. Bio Mater.*, 2019, **2**, 4571–4582.
82 M. B. Akolpoglu, N. O. Dogan, U. Bozuyuk, H. Ceylan, S. Kizilel and M. Sitti, *Adv. Sci.*, 2020, **7**, 2001256.
83 H. Choi, B. Kim, S. H. Jeong, T. Y. Kim, D. Kim, Y. Oh and S. K. Hahn, *Small*, 2023, **19**, 2204617.
84 I. S. Shchelik, J. V. D. Molino and K. Gademann, *Acta Biomater.*, 2021, **136**, 99–110.
85 T. Studer, D. Morina, I. S. Shchelik and K. Gademann, *Chem. – Eur. J.*, 2023, **29**, e202203913.
86 F. Zhang, J. Zhuang, Z. Li, H. Gong, B. E.-F. de Ávila, Y. Duan, Q. Zhang, J. Zhou, L. Yin, E. Karshalev, W. Gao, V. Nizet, R. H. Fang, L. Zhang and J. Wang, *Nat. Mater.*, 2022, **21**, 1324–1332.
87 F. Zhang, Z. Li, Y. Duan, A. Abbas, R. Mundaca-Uribe, L. Yin, H. Luan, W. Gao, R. H. Fang, L. Zhang and J. Wang, *Sci. Rob.*, 2022, **7**, eabo4160.
88 F. Zhang, Z. Li, Y. Duan, H. Luan, L. Yin, Z. Guo, C. Chen, M. Xu, W. Gao, R. H. Fang, L. Zhang and J. Wang, *Sci. Adv.*, 2022, **8**, eade6455.
89 F. Zhang, Z. Li, L. Yin, Q. Zhang, N. Askarinam, R. Mundaca-Uribe, F. Tehrani, E. Karshalev, W. Gao, L. Zhang and J. Wang, *J. Am. Chem. Soc.*, 2021, **143**, 12194–12201.
90 J. Lai, Q.-F. Meng, M. Tian, X. Zhuang, P. Pan, L. Du, L. Deng, J. Tang, N. Jin and L. Rao, *Cell Rep. Phys. Sci.*, 2022, **3**, 101061.
91 F. Mushtaq, X. Chen, S. Staufert, H. Torlakcik, X. Wang, M. Hoop, A. Gerber, X. Li, J. Cai, B. J. Nelson and S. Pané, *J. Mater. Chem. A*, 2019, **7**, 24847–24856.
92 X. Yan, J. Xu, Q. Zhou, D. Jin, C. I. Vong, Q. Feng, D. H. L. Ng, L. Bian and L. Zhang, *Appl. Mater. Today*, 2019, **15**, 242–251.
93 D. Gong, N. Celi, L. Xu, D. Zhang and J. Cai, *Mater. Today Chem.*, 2022, **23**, 100694.
94 C. Zheng, Z. Li, T. Xu, L. Chen, F. Fang, D. Wang, P. Dai, Q. Wang, X. Wu and X. Yan, *Appl. Mater. Today*, 2021, **22**, 100962.
95 D. Zhong, W. Li, Y. Qi, J. He and M. Zhou, *Adv. Funct. Mater.*, 2020, **30**, 1910395.
96 M. Hosseini, Z. Ahmadi, A. Kefayat, F. Molaabasi, A. Ebrahimpour, Y. Naderi Khojasteh Far and M. Khoobi, *ACS Appl. Mater. Interfaces*, 2022, **14**, 37447–37465.
97 D. Zhang, D. Zhong, J. Ouyang, J. He, Y. Qi, W. Chen, X. Zhang, W. Tao and M. Zhou, *Nat. Commun.*, 2022, **13**, 1413.
98 L. Liu, B. Chen, K. Liu, J. Gao, Y. Ye, Z. Wang, N. Qin, D. A. Wilson, Y. Tu and F. Peng, *Adv. Funct. Mater.*, 2020, **30**, 1910108.
99 L. Liu, J. Wu, S. Wang, L. Kun, J. Gao, B. Chen, Y. Ye, F. Wang, F. Tong, J. Jiang, J. Ou, D. A. Wilson, Y. Tu and F. Peng, *Nano Lett.*, 2021, **21**, 3518–3526.
100 X. Yan, Q. Zhou, M. Vincent, Y. Deng, J. Yu, J. Xu, T. Xu, T. Tang, L. Bian, Y.-X. J. Wang, K. Kostarelos and L. Zhang, *Sci. Rob.*, 2017, **2**, eaaq1155.
101 Y. X. J. Wáng and J.-M. Idée, *Quant. Imaging Med. Surg.*, 2017, **7**, 88–122.
102 L. Xu, D. Gong, N. Celi, J. Xu, D. Zhang and J. Cai, *Appl. Surf. Sci.*, 2022, **579**, 152165.
103 H. Wang, H. Liu, Y. Guo, W. Zai, X. Li, W. Xiong, X. Zhao, Y. Yao, Y. Hu, Z. Zou and J. Wu, *Bioact. Mater.*, 2022, **12**, 97–106.
104 Y. Qiao, F. Yang, T. Xie, Z. Du, D. Zhong, Y. Qi, Y. Li, W. Li, Z. Lu, J. Rao, Y. Sun and M. Zhou, *Sci. Adv.*, 2020, **6**, eaba5996.
105 D. Zhong, W. Li, S. Hua, Y. Qi, T. Xie, Y. Qiao and M. Zhou, *Theranostics*, 2021, **11**, 3580–3594.
106 L. Liu, J. Wu, B. Chen, J. Gao, T. Li, Y. Ye, H. Tian, S. Wang, F. Wang, J. Jiang, J. Ou, F. Tong, F. Peng and Y. Tu, *ACS Nano*, 2022, **16**, 6515–6526.
107 M. Li, J. Wu, D. Lin, J. Yang, N. Jiao, Y. Wang and L. Liu, *Acta Biomater.*, 2022, **154**, 443–453.
108 A. Panda, A. S. Reddy, S. Venkateswarlu and M. Yoon, *Nanoscale*, 2018, **10**, 16268–16277.
109 J. Wang, F. Soto, S. Liu, Q. Yin, E. Purcell, Y. Zeng, E. Hsu, D. Akin, B. Sinclair, T. Stoyanova and U. Demirci, *Adv. Funct. Mater.*, 2022, **32**, 2201800.
110 H. Chen, Y. Li, Y. Wang, P. Ning, Y. Shen, X. Wei, Q. Feng, Y. Liu, Z. Li, C. Xu, S. Huang, C. Deng, P. Wang and Y. Cheng, *ACS Nano*, 2022, **16**, 6118–6133.
111 M. B. Akolpoglu, Y. Alapan, N. O. Dogan, S. F. Baltaci, O. Yasa, G. Aybar Tural and M. Sitti, *Sci. Adv.*, 2022, **8**, eabo6163.
112 M. Yang, M. Conceição, W. Chen, F. Yang, B. Zhao, M. J. A. Wood, L. Qiu and J. Chen, *Acta Biomater.*, 2023, **158**, 734–746.
113 T. Wang, Q. Yin, H. Y. Huang, Z. Wang, H. Song and X. Luo, *Colloids Surf., B*, 2023, **225**, 113277.
114 S. Xie, C. Mo, W. Cao, S. Xie, S. Li, Z. Zhang and X. Li, *Acta Biomater.*, 2022, **142**, 49–59.
115 O. I. Sentürk, O. Schauer, F. Chen, V. Sourjik and S. V. Wegner, *Adv. Healthcare Mater.*, 2020, **9**, 1900956.
116 Y. Li, S. Tang, Z. Cong, D. Lu, Q. Yang, Q. Chen, X. Zhang and S. Wu, *Mater. Today Chem.*, 2022, **23**, 100609.
117 X. Zeng, P. Li, S. Yan and B.-F. Liu, *Chem. Eng. J.*, 2023, **452**, 139517.
118 S. Xie, P. Zhang, Z. Zhang, Y. Liu, M. Chen, S. Li and X. Li, *Acta Biomater.*, 2021, **131**, 172–184.
119 S. Xie, S. Li, W. Cao, C. Mo, Z. Zhang, K. Huang and X. Li, *ACS Appl. Mater. Interfaces*, 2022, **14**, 37553–37565.
120 J. Zhou, E. Karshalev, R. Mundaca-Uribe, B. Esteban–Fernández de Ávila, N. Krishnan, C. Xiao, C. J. Ventura, H. Gong, Q. Zhang, W. Gao, R. H. Fang, J. Wang and L. Zhang, *Adv. Mater.*, 2021, **33**, 2103505.
121 S. Xiao, H. Shi, Y. Zhang, Y. Fan, L. Wang, L. Xiang, Y. Liu, L. Zhao and S. Fu, *J. Nanobiotechnol.*, 2022, **20**, 178.
122 W. Li, Z. Zhang, J. Liu, B. Wang, G. Pu, J. Li, Y. Huang and M. Chu, *Acta Biomater.*, 2022, **146**, 341–356.
123 S. Reghu and E. Miyako, *Nano Lett.*, 2022, **22**, 1880–1888.

124 C. Chen, Y. Wang, Y. Tang, L. Wang, F. Jiang, Y. Luo, X. Gao, P. Li and J. Zou, *Int. J. Hyperthermia*, 2020, **37**, 870–878.
125 S.-J. Song, C. C. Mayorga-Martinez, J. Vyskočil, M. Častorálová, T. Ruml and M. Pumera, *ACS Appl. Mater. Interfaces*, 2023, **15**, 7023–7029.
126 T. Gwisai, N. Mirkhani, M. G. Christiansen, T. T. Nguyen, V. Ling and S. Schuerle, *Sci. Rob.*, 2022, **7**, eabo0665.
127 C. Chen, P. Wang, H. Chen, X. Wang, M. N. Halgamuge, C. Chen and T. Song, *ACS Appl. Mater. Interfaces*, 2022, **14**, 14049–14058.
128 B. Wang, Y. Qin, J. Liu, Z. Zhang, W. Li, G. Pu, Z. Yuanhe, X. Gui and M. Chu, *ACS Appl. Mater. Interfaces*, 2023, **15**, 2747–2759.
129 D. Lu, S. Tang, Y. Li, Z. Cong, X. Zhang and S. Wu, *Micromachines*, 2021, **12**, 797.
130 B. Zhang, H. Pan, Z. Chen, T. Yin, M. Zheng and L. Cai, *Sci. Adv.*, 2023, **9**, eadc8978.
131 L. Zhang, B. Zhang, R. Liang, H. Ran, D. Zhu, J. Ren, L. Liu, A. Ma and L. Cai, *ACS Nano*, 2023, **17**, 6410–6422.
132 R. Maria-Hormigos, C. C. Mayorga-Martinez, T. Kinčl and M. Pumera, *ACS Nano*, 2023, **17**, 7595–7603.
133 S. Wang, H. Chen, Z. Xu, X. Wang, Z. Tao, L. Wang, X. Liu and X. Huang, *ACS Appl. Nano Mater.*, 2023, **6**, 4626–4635.
134 T. Bhuyan, A. K. Singh, S. S. Ghosh and D. Bandyopadhyay, *Bull. Mater. Sci.*, 2020, **43**, 111.
135 T. Bhuyan, A. K. Singh, D. Dutta, A. Unal, S. S. Ghosh and D. Bandyopadhyay, *ACS Biomater. Sci. Eng.*, 2017, **3**, 1627–1640.
136 Y. Zhang, K. Yan, F. Ji and L. Zhang, *Adv. Funct. Mater.*, 2018, **28**, 1806340.
137 F. Striggow, M. Medina-Sánchez, G. K. Auernhammer, V. Magdanz, B. M. Friedrich and O. G. Schmidt, *Small*, 2020, **16**, 2000213.
138 R. Luthfikasari, T. V. Patil, D. K. Patel, S. D. Dutta, K. Ganguly, M. M. Espinal and K. Lim, *Small*, 2022, **18**, 2201417.
139 Y. Chen, W. Xu, H. Tian, J. Gao, Y. Ye, H. Qin, H. Wang, Y. Song, C. Shao, F. Peng and Y. Tu, *ACS Appl. Mater. Interfaces*, 2024, **16**, 39051–39063.
140 L. Chen, Q. Gan, X. Xiao, S. Cai, X. Yan and C. Zheng, *J. Mater. Sci.*, 2024, **59**, 4267–4280.
141 M. Zhang, S. Yang, W. Zhong, H. Wang, U. T. Uthappa and B. Wang, *Chem. Eng. J.*, 2024, **495**, 153264.
142 G. Xing, X. Yu, Y. Zhang, S. Sheng, L. Jin, D. Zhu, L. Mei, X. Dong and F. Lv, *Small*, 2024, **20**, 2305526.
143 G. Go, S.-G. Jeong, A. Yoo, J. Han, B. Kang, S. Kim, K. T. Nguyen, Z. Jin, C.-S. Kim, Y. R. Seo, J. Y. Kang, J. Y. Na, E. K. Song, Y. Jeong, J. K. Seon, J.-O. Park and E. Choi, *Sci. Rob.*, 2020, **5**, eaay6626.
144 H. Huang, J. Li, C. Wang, L. Xing, H. Cao, C. Wang, C. Y. Leung, Z. Li, Y. Xi, H. Tian, F. Li and D. Sun, *Small*, 2024, **20**, 2304088.
145 B. Wang, Y. Qin, J. Liu, Z. Zhang, W. Li, G. Pu, Z. Yuanhe, X. Gui and M. Chu, *ACS Appl. Mater. Interfaces*, 2023, **15**, 2747–2759.
146 C. Chen, P. Wang, H. Chen, X. Wang, M. N. Halgamuge, C. Chen and T. Song, *ACS Appl. Mater. Interfaces*, 2022, **14**, 14049–14058.
147 Y. Yao, J. Li, P. Li, D. Wang, W. Bao, Y. Xiao, X. Chen, S. He, J. Hu and X. Yang, *Small*, 2022, **18**, 2105716.
148 T. Gwisai, N. Mirkhani, M. G. Christiansen, T. T. Nguyen, V. Ling and S. Schuerle, *Sci. Rob.*, 2022, **7**, eabo0665.
149 Y. Zhang, L. Zhang, L. Yang, C. I. Vong, K. F. Chan, W. K. K. Wu, T. N. Y. Kwong, N. W. S. Lo, M. Ip, S. H. Wong, J. J. Y. Sung, P. W. Y. Chiu and L. Zhang, *Sci. Adv.*, 2019, **5**, eaau9650.